Republic of Iraq
Ministry of Higher Education
and Scientific Research
University of Babylon
College of Materials Engineering
Department of Metallurgical Engineering

Investigation the Effect of Heat treatment and Warm Squeezing on the Machinability of AA7075 Alloy Prepared by Casting

A Thesis

Submitted to the Council of the College of Materials Engineering/ University of Babylon in Partial Fulfillment of the Requirements for the Master of Degree in Materials Engineering / Metallurgical

By

Mohammed Almahdi Hatef Almohanna

(B.Sc. in Metals Engineering)

(2018-2019)

Supervised by

Prof. Haydar Al-Ethari (Ph.D.)

Asst. Prof. Talib A. Jasim

2023 A.D **1444 A.H**

وزارة التعليم العالي والبحث العلمي
جامعـــــــــــة بابـــــــــــل
كليـــــــــة هنـــــــــــدسة المواد
قسم هنـــــــــــدسة المعادن

البحث في تأثير المعاملات الحرارية والعصر الدافئ على قابلية تشغيل سبيكة AA7075 المحضرة بالسباكة

رسالة

مقدمة إلى قسم المعادن في كلية هندسة المواد / جامعة بابل وهي جزء من متطلبات نيل درجة الماجستير في علوم

هندسة المواد/ معادن

من قبل

محمد المهدي هاتف يامرالمحنة

(بكالوريوس هندسة معادن)

(٢٠١٨-٢٠١٩)

بإشراف

أ.د. حيدر عبد الحسن حسين العذاري

أ.م. طالب عبد الامير جاسم

م / ٢٠٢٣ **هـ/١٤٤٣**

بِسْمِ اللَّهِ الرَّحْمَٰنِ الرَّحِيمِ

يَرْفَعِ اللَّهُ الَّذِينَ آمَنُوا مِنكُمْ وَالَّذِينَ أُوتُوا الْعِلْمَ
دَرَجَاتٍ وَاللَّهُ بِمَا تَعْمَلُونَ خَبِيرٌ

صدق اللّٰهُ العلي العظيم

(سورة المجادلة–اية ١١)

Dedication

Heartfelt appreciation and gratitude to all those who have contributed to the completion of this work.

Mohammed Almahdi

2023

Acknowledgments

All thanks to **Allah** for his grace and mercy that enabled me to complete this work.

I want to express my utmost gratitude to my supervisors, **Prof. Dr. Haydar Al-Ethari and Asst. Prof. Talib A. Jasim**, for their valuable guidance, expertise, and unwavering support throughout the process of conducting this study and for their constant encouragement that have played a significant role in shaping the trajectory of this study.

Sincere gratitude to the Materials Engineering College for their constant assistance.

I am also grateful to my family and friends who supported me and stood by me at all stages. They were a source of strength and inspiration to me, for whom I am very grateful.

Mohammed Almahdi

2023

Supervisors, Certification

We confirm that the thesis titled **" Investigation of the Effect of Heat Treatment and Warm Squeezing on the Machinability of AA7075 Al Alloy Prepared by Casting "** has been conducted by **(Mohammed Almahdi Hatef Almohanna)**

under our guidance at the Department of Metallurgical Engineering, Faculty of Materials Engineering/ University of Babylon/ as a requirement for the degree of Master of Science in Materials Engineering.

Signature:
Name: : Prof. Dr. Haydar Al-Ethari
(supervisor)
Date: / / 2023

Signature:
Name Asst. Prof. Talib A. Jasim
(supervisor)
Date: / / 2023

الخلاصة:

ركزت هذه الدراسة على سبيكة 7075 المنيوم نظرا لخصائصها الفريدة مثل التركيبة خفيفة الوزن والخصائص الميكانيكية المحسنة وسهولة التشغيل والتشكيل. كانت هذه الصفات كافيه لتلبية المتطلبات المتنوعة للصناعات والتطبيقات المختلفة ، مما يجعل هذه السبائك الموضوع الرئيسي للتحقيق في هذا البحث. تم فحص البنية المجهرية للسبائك ، والصلادة ، والمسامية ، والكثافة ، بالإضافة إلى متوسط قطر الحبيبات ، وقوة القطع ، والخشونة السطحية ، ونسبة الاستطالة في اختبار الشد. كما تم فحص تأثير المعالجة الحرارية والعصر الدافئ على هذه الخصائص. لتحضير العينات، تم استخدام الصب باستخدام فرن غاز وجو غاز خامل .تم اجراء المعالجة الحرارية والعصر الدافئ لتعزيز الخصائص المحددة للعينات المصبوبة. تعرضت السبيكة لعملية عصر عند درجة حرارة (120°C) لمدة (10 min) لكل عملية عصر ، بأستخدام قيم ضغط مختلفة (95, 110, 140 MPa).

كشفت نتائج المعالجة الحرارية أن قيم صلاده برينل وفيكرز تبلغ ($145, 156 kg/ mm^2$) على التوالي زادت إلى ($178 and 209 kg/ mm^2$). تم تحديد المسامية لتكون(12%)، بينما كانت الكثافة (2.76 g/ cm3) ولكن بعد العصر سجلت هذه الخصائص قيم انخفاض في المسامية إلى (4 %) وزيادة في الكثافة إلى (2.98 g/ cm3) على التوالي. بالإضافة إلى ذلك ، تم الكشف على متوسط قطر الحبيبات ليكون (962nm) بأستخدام مجهر القوة الذرية ، ولكن مع تأثير تطبيق العصر الدافئ ، أنخفض متوسط قطر الحبيبات كما لوحظ من خلال مجهر القوة الذرية ، إلى (655nm). أيضا شهدت نسبة الاستطالة للعينة المعالجة حراريا زيادة بنسبة (11%)، ومع التعرض للعصر الدافئ ، زادت نسبة الاستطالة بنسبة (40%)، وأرتفعت هذه النسبة مع زيادة درجة الحرارة. خاصة عند درجات حرارة (200°C, 250°C, 300°C)، وصلت النسبة المئوية إلى (62%, 94%, 191%) على التوالي. في المقابل ، أظهرت العينة المعالجة حراريا فقط نسبة استطالة تبلغ (162%) عند درجة حرارة (300°C).

تم أستخدام عينتين أيضا لمزيد من التجارب: خضعت إحداهما للمعالجة الحرارية فقط ، بينما خضعت الأخرى للمعالجة الحرارية والعصر الدافئ عند (140 MPa). تعرضت كل عينة لثلاث سرعات قطع (7, 14, 52 m/ min) ومعدلين للتغذية (0.130, 0.70 mm/rev). في العينة الأولى ، عند استخدام معدل تغذية (0.130 mm/rev) ، تم قياس قيم الخشونة على أنها (1.181, 0.952, 0.801 µm) ، وبمعدل تغذية (0.70 mm/rev)، كانت قيم الخشونة

(2.976, 2.428, 1.853 µm). تم تحديد قوة القطع ، تحت معدل تغذية (0.130 mm/rev) ، لتكون (12, 14, 17 N) ، بينما مع معدل تغذية (0.70 mm/rev) ، كانت قيم قوة القطع (9, 12, 14 N). أما بالنسبة للعينة الثانية التي تم ضغطها بمقدار(140 MPa) ، عند التغذية (0.130 mm/rev)، أنخفضت الخشونة إلى (0.824, 0.653, 0.481µm) ، وبمعدل تغذية (0.70 mm/rev) ، أنخفضت أيضا إلى (1.992, 1.559, 1.001 µm) ، بينما زادت قوة القطع عند التغذية (0.130 mm/rev) إلى (8, 9, 13 N) وعند التغذية (0.70 mm/rev) إلى (6, 8, 10 N).

Abstract

This research primarily focused on the 7075Al alloy, which possesses unique characteristics like its lightweight composition, improved mechanical properties, and ease of machining and forming. These attributes are essential for meeting the diverse requirements of various industries and applications, making this alloy the central subject of investigation.

The study examined the alloy's microstructure, hardness, porosity, density, grain size, cutting force, surface roughness, and elongation percentage in tensile tests. The impact of heat treatment and warm squeezing on these properties was also investigated. To create alloy samples, stir casting was used, employing a gas furnace and an inert gas atmosphere. Heat treatment and warm squeezing were applied to enhance specific characteristics of the cast alloy sample. The material underwent a squeezing process at (120°C) for (10 min), with various pressure values (95, 110, and 140 MPa).

The results of the heat treatment showed that the Brinell and Vickers hardness values increased from (145 and 156 kg/ mm^2) to (178 and 209 kg/ mm^2), respectively. Porosity decreased from (12%) to (4%), and density increased from (2.76 g/ cm^3) to (2.98 g/ cm^3) after squeezing. The average grain size, observed with an atomic force microscope, decreased from (962 nm) to (655 nm) due to warm squeezing. The percentage of elongation increased by (11%) with heat treatment and by (40%) with warm squeezing, further rising with increased temperature (62%, 94%, and 191% at 200°C, 250°C, and 300°C, respectively). In contrast, the heat-treated sample alone exhibited an elongation percentage of (162% at 300°C).

Two samples were used for further experimentation**:** one underwent only heat treatment, while the other underwent both heat treatment and warm squeezing at 140 MPa. Each sample was subjected to three cutting speeds (7, 14, 52 m/min) and two feed rates (0.130, 0.70 mm/rev). In the first sample, with a feed rate of (0.130 mm/rev), the roughness values were measured at (1.181, 0.952, and 0.801µm), while at a feed rate of (0.70 mm/rev), the roughness values were (2.976, 2.428, and 1.853 µm). The cutting force, with a feed rate of (0.130 mm/rev), was (12, 14, and 17N), and with a feed rate of (0.70 mm/rev), it was (9, 12, and 14N). As for the second sample squeezed at (140 MPa), the roughness decreased to (0.824, 0.653, and 0.481µm) at a feed rate of (0.130 mm/rev) and to (1.992, 1.559, and 1.00 µm) at a feed rate of (0.70 mm/rev). The cutting force increased to (6, 8, and 10N), at a feeding of (0.130 mm/rev) and to (8, 9, and 13N) at a feeding of (0.70 mm/rev).

Table of Contents

List of Tables

Table of Figures

List of Abbreviations

symbols	*Description*	*Unit*
α	**Alpha Phase**	**-**
Ra	**Arithmetic Mean Value of Surface Roughness**	**µm**
β	**Beta Phase**	**-**
ρ	**Density**	**g/cm^3**
d	**Depth of Cut**	**mm**
f	**Feed Rate**	**mm/sec**
T	**Temperature**	**°C**
t	**Time**	**sec**
n	**Spindle Speed**	**rpm**
σ	**Stress**	**(N/m^2)**
m	**Strain-rate Sensitivity**	**-**

Chapter One

Chapter One

Introduction

1.1 Overview

The need for high-strength, lightweight structural elements has been growing over the past several years as a result of the fast advancements in big aircraft, high-speed trains, and aerospace engineering. Structures made of lightweight, high-strength alloys can enhance material attributes. High-strength aluminium alloys are utilized extensively in the aerospace sector and offer the benefits of low density and high strength. High-strength aluminium alloys' weak ductility at room temperature, however, restricts their use[1].

Using alloying elements in aluminium enhances mechanical properties such as machinability, stiffness, hardness, and tensile strength, and occasionally enhances fluidity and other casting aspects[2]. Aluminium alloys for sheet metal provide excellent candidates for usage in the automotive sector due to their excellent strength and strength-to-weight ratios. The limited formability of aluminium sheet alloys at room temperature restricts the design uses for these materials. Aluminium alloys are often employed in structural sections of aeroplanes and are frequently used in highly strained functional applications. These alloys' formability can be greatly enhanced by warm forming[3]. The major alloying ingredient in 7075 is zinc. It serves as the main alloying ingredient in the aluminium (7075) alloy. Moreover, it possesses exceptional mechanical properties, including toughness, high strength, great fatigue resistance, and most critically, superb corrosion resistance. When magnesium is added, MgZn2 is formed, which has a significant strengthening effect. This

alloy has a significantly greater heat treatment effect than binary alloys made of aluminium and zinc. The tensile strength of the alloy will rise with an increase in zinc and magnesium content, but it will lose some of its resistance to stress corrosion and fragmentation corrosion. It may attain very high strength qualities with thermal treatment [4].

There is a very big demand for new and innovative aluminium alloy products that meet the ever-changing demands of the market. One such big challenge for manufacturers today is to achieve higher performance and more functional characteristics resulting from the increased choice of design options as well as processing variants that are becoming available in the market [5].

Alloy 7075 aluminium has some operational problems, including poor formability at room temperature, which limits its usefulness in certain manufacturing processes. This is due to its high strength and low ductility, which makes it difficult to form complex shapes without cracking or tearing. However, the warm squeezing process can help improve its plasticity by reducing the likelihood of cracking and enhancing its ductility making it easier to form into complex shapes[6, 7]. As well, many applications of this alloy need higher machining properties like accuracy and machined surface quality. This is achieved by more stable machinability as a result of increased homogeneity of microstructure.

1.2 Applications of 7075 Al Alloy

The 7075 aluminium alloy is a good choice for applications that call for lightweight components with the highest level of strength available. The 7075 aluminium alloy also enables highly precise fabrication of extremely complicated shapes. Applications for 7075 aluminium components are frequently used in the aerospace, aviation, and automotive sectors. 7075 aluminium components are frequently utilized in structures and many elements need a high strength-to-weight ratio [8, 9], as depicted in Figure (1.1).

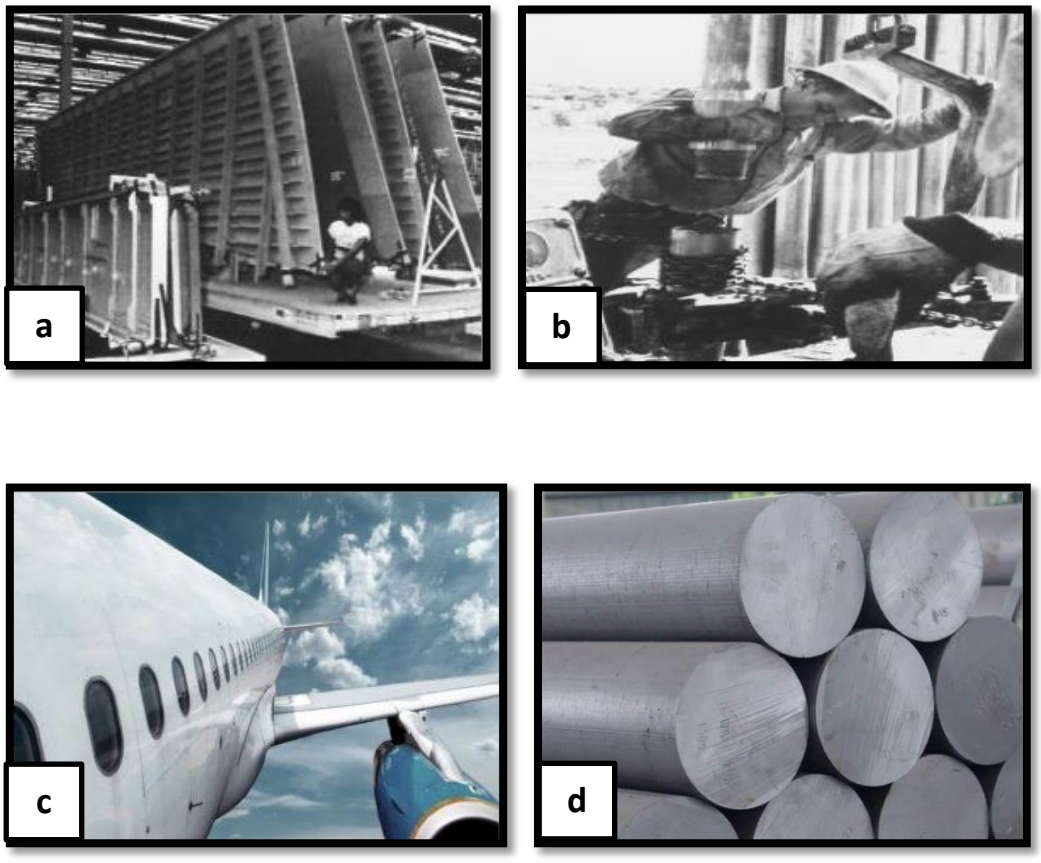

Figure(1.1)**:** Applications of Al-Zn-Mg Alloys in; (a) Critical Aircraft Wing Structures; (b) Long-length Drill Pipes; (c) Airplane Wings; (d) Round Bars[8]

1.2 Objectives of the Present Study

The study focuses on improving the performance of 7075 aluminium alloy by using warm squeezing. Systematic examination of different tests is conducted with the following objectives**:**

1. Evaluate the enhancement of metallurgical and mechanical properties in 7075 aluminium alloys.
2. Investigate various properties, including microstructure, porosity, density, grain size, hardness, superplasticity, tensile strength, and machining characteristics.
3. Clarify the effect of heat treatments and warm squeezing on these properties.

Chapter Two

Chapter Two

Theoretical Background and Literature Review

2.1 Introduction

This chapter presents a summary of aluminium, its alloys, methods of production and classification, and discusses superplastic alloys. The chapter also provides an analysis of grain refining techniques, including the method of grain refinement by grain squeezing and the effect of plastic deformation on the mechanical properties of the alloys. The chapter provides a literature review including information on mechanical grain compaction with in-process temperature control and some grain refining techniques, as well as scaling up of superplastic alloys, and the influence on the machining properties.

2.2. Aluminium and Its Alloys

Aluminium is a lightweight, silver-hued metal with a low melting point of 660°C, and it is known for its softness. Aluminium is considered one of the most prominent economical and service metals for many groups of engineering applications and the second most abundant element on earth. Its density is about 2.7 g/cm^3, which is equivalent to about one-third of the steel [9, 10]. Some Aluminium alloys exceed steel in strength. This high strength of some alloys, which are combined with lightweight, helps to accomplish and build large, lightweight and high-strength structures[11]. Aluminium is important in engineering applications that require high protection against corrosion as It resists oxidation due to the formation of a very thin oxide shell on its surface.

One of the advantages of Aluminium is that it has high electrical and thermal conductivity, also considered non-magnetic, so it is important in the electrical and electronic industries[12]. Aluminium accepts the formation on cold and easily hardened and as a result the tensile strength increases. Aluminium casting and structures can be manufactured in any way from metal production methods such as casting, drawing, rolling and other methods adopted taking into account the production conditions of temperature, amount of power used, required design and other requirements to be provided for the production of Aluminium. The alloys of this element are also characterized by superior flexibility, which through this feature can produce complex shapes and precise designs with ease and high accuracy. These alloys also accept different heat treatments that allow the designer to choose the required property from durability, lengthening and other required engineering characteristics and problems in production[13].

2.3 Designation and Classification of Aluminium Alloys

The Aluminium alloy core can be categorized into two primary groups: cast alloys and wrought alloys. Each group displays distinct variations in their properties based on the specific method used to enhance them. One crucial factor in modifying the properties of many alloys is thermal treatment, which relies on the solubility of different phases. These treatments encompass various processes, including solution heat treatment, rapid cooling (quenching), precipitation, and age hardening. Alloys that can undergo these processes are termed "heat treatable," and this applies to both wrought and casting alloys. On the other hand, a significant number of wrought alloys rely on mechanical

reductions for work hardening, making them "hardenable" and "workable" alloys. It's important to note that many casting alloys are not amenable to heat treatment[14].

2.3.1 Wrought Aluminium Alloys

Aluminium wrought alloys are a type of aluminium alloy that contains Aluminium as the dominant metal. These alloys find their primary utility in manufacturing processes like rolling and extrusion. Additionally, this particular type of Aluminium alloy can be categorized into two main groups: heat-treatable alloys and non-heat-treatable alloys. Heat-treated alloys can be strengthened through heat-treatment procedures [15]. The primary strength of these alloys is derived from alloying elements like copper, silicon, magnesium, and zinc. On the other hand, alloys that are not amenable to heat treatment cannot be strengthened through this process. Their initial strength is attributed to alloying elements such as manganese, silicon, and magnesium. Since heat treatment is ineffective, these alloys can be strengthened through cold working or strain hardening [16]. Notably, the key distinction between cast and wrought Aluminium alloys lies in the presence of numerous internal and external defects in cast Aluminium alloys, whereas wrought Aluminium alloys are typically devoid of such defects. A system of four-digit numbers is employed to classify wrought Aluminium and its alloys[15].

Aluminium alloys are classified based on their composition, which includes the primary alloying element and any secondary elements that are added. The most commonly used classification system for

Aluminium alloys is the Aluminium Association (AA) system, which is based on a four-digit numbering system.

The first digit in the AA system indicates the major alloying element, as follows**:**

- **1xxx:** Pure Aluminium.
- **2xxx :** Copper.
- **3xxx :** Manganese.
- **4xxx :** Silicon.
- **5xxx :** Magnesium.
- **6xxx:** Magnesium and silicon.
- **7xxx :** Zinc.
- **8xxx:** Other elements, such as tin or lithium.

In the AA system, the second digit is used to denote any alterations or changes that have been implemented to the alloy, such as the addition of other elements, while the last two digits provide specific information about the composition and processing of the alloy.

There are other classification systems used for Aluminium alloys, such as the Unified Numbering System (UNS) and the International Alloy Designation System (IADS), but the AA system is the most commonly used[17]. The 7075-T6 Aluminium alloy belongs to the 7000 series and is recognized for its excellent balance between strength and weight. It is commonly used in aerospace and military applications. The "-T6" designation refers to the temper or heat treatment that the alloy has undergone. The T6 temper involves solution heat treatment, quenching, and artificial ageing, which results in very high strength and toughness [18].

2.3.2 Cast Aluminium Alloys

The cast alloys of Aluminium provide relatively low melting temperatures compared with cast iron or steel, they also contain minimal gas solubility except for hydrogen, good fluidity and smooth surface finishing. However, cast alloys suffer from severe shrinkage reaching up to 7 % throughout the solidification process. Better mechanical characteristics can be obtained in these alloys by controlling the impurities amount, size of grain and solidification parameters e.g. cooling rate. The identification of Aluminium and its alloys, whether in the form of castings or foundry ingots, employs a numerical system comprising four digits, which includes a decimal point. Aluminium ingots can be classified into different categories based on their composition and properties[19, 20].

2.4 Solidification of Al-Zn-Mg Alloy

The 7000 series alloys, based on Aluminium-zinc compositions, exhibit fundamental differences in solidification. Aluminium metal has a face-centred cubic structure and is rather anisotropic, while zinc has a hexagonal and not very anisotropic structure. This discrepancy in anisotropy results in changes in interfacial energy, which impact the growth direction and morphology of dendrites. These alloys are saturated solid solutions that gradually disintegrate and begin to achieve an equilibrium state [21, 22]. The Al-Zn system also displays a positive heat of mixing, and at 20 ºC, the solubility of zinc in Aluminium is less than 2wt. %, as illustrated in Figure (2.1).

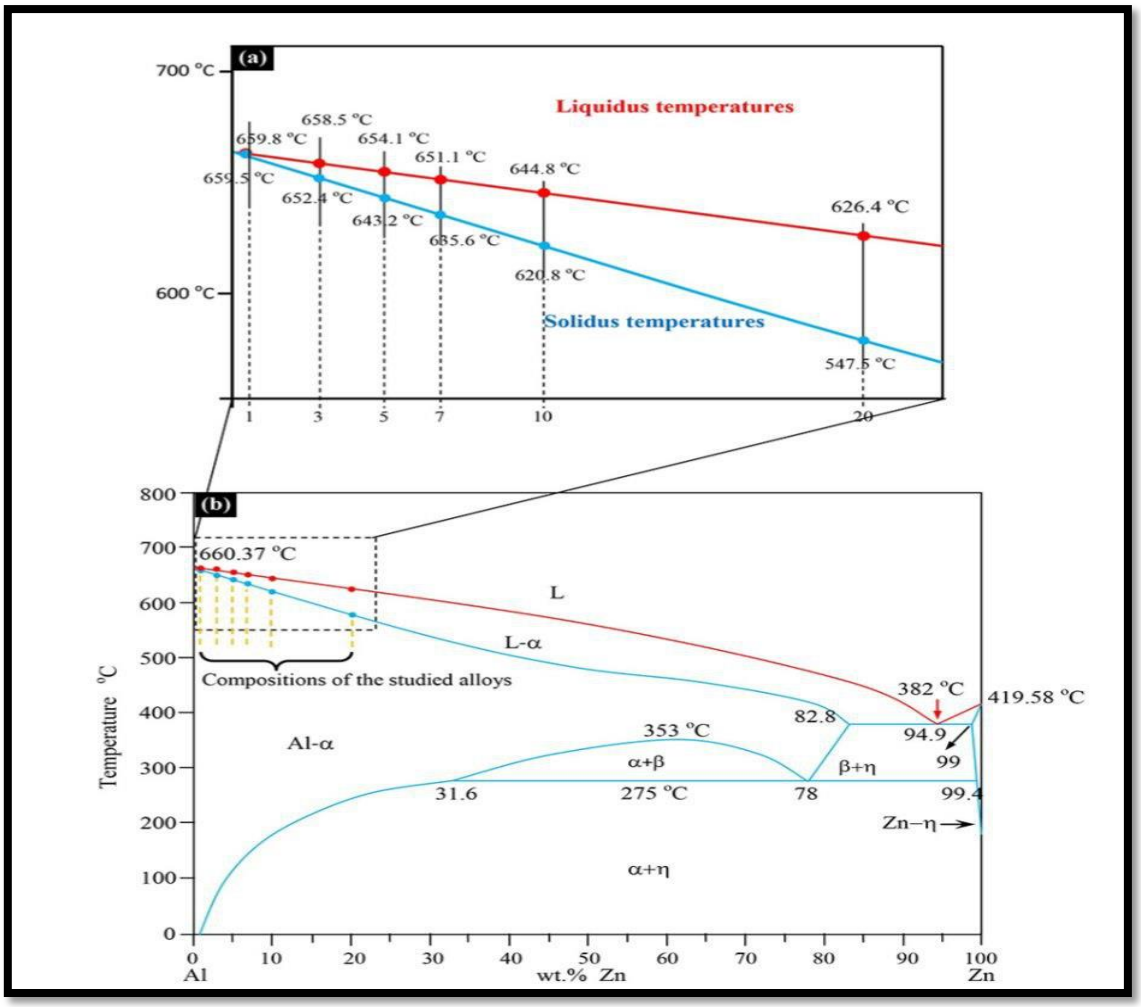

Figure (2.1)**:** Phase Diagram of the Zinc System (a) Partial Image (b) Full Image[23]

Many studies of this type of binary Al-Zn alloys have shown that the Zn content and applied cooling rate interact to produce different final morphologies in the Al-Zn alloys. As the contact between the atoms of Al and Zn is very weak, intermetallic phases between Al and Zn do not occur at lower Zn contents, which means that for alloys with less than 40% Zn, intermetallic phases between Al and Zn are not expected to form. Because the analyzed alloys' Zn concentration is minimal [232].

During the casting process, after melting the 7075 Aluminium alloy, it is subsequently poured into a mould where it undergoes the process of cooling and solidification. The properties of the alloy's structure and

mechanical characteristics can be influenced by the speed at which it solidifies, cools down, and the temperature of the mould. To optimize the solidification process, it is important to use the appropriate mould materials and preheat the mould to the correct temperature. Overall, the solidification process of 7075 Aluminium alloy is an important consideration for achieving the desired properties and performance of the material. Careful control of the process parameters can ensure optimal microstructure and mechanical properties [24, 25].

2.5 Al-Zn Phase Diagram

Based on the binary equilibrium diagram of (Al-Zn) shown in Figure (2.2), the presence of solute solubility leads to a reduction in the solubility of the solid solution as the temperature decreases.

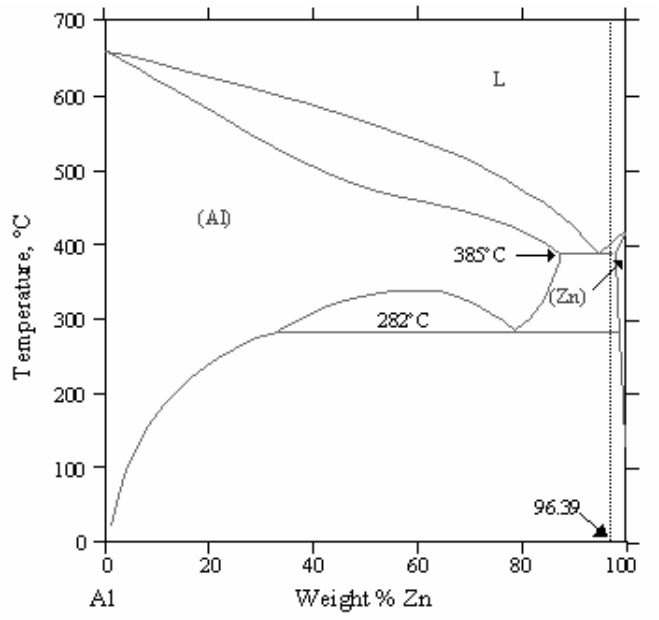

Figure (2.2)**:** The Al-Zn Equilibrium Phase Diagram [26]

The Al-Zn phase diagram shows the phases that form when Aluminium (Al) and zinc (Zn) are combined at different temperatures and compositions. The diagram is useful for understanding the properties of alloys made from these two metals.

At low temperatures and low zinc concentrations, the alloy is a solid solution of zinc in Aluminium, known as the alpha phase (α). As the temperature increases or the zinc concentration increases, a second phase, known as the eta phase (η), can form. The eta phase is a complex intermetallic compound of Aluminium and zinc with a hexagonal crystal structure. At higher temperatures, the alpha phase becomes unstable and transforms into a different solid solution, called the beta phase (β), which has a face-centered cubic crystal structure. The beta phase can also contain small amounts of zinc-rich intermetallic compounds, such as Al3Zn and Al Zn. The phase diagram also shows the melting points of the different phases, as well as the eutectic point, which is the temperature and composition at which the liquid phase transforms into a mixture of alpha and eta phases during cooling[26].

Overall, the Al-Zn phase diagram provides important information for the design and production of Aluminium-zinc alloys with specific properties, such as strength, ductility, and corrosion resistance. Also, the transformations that define the topology are summarized in the diagram Table (2.1).

Table (2.1)**:** Special Points in the Al-Zn Phase Diagram[27]

Phase	Composition, at. %(Zn)	Temp, °C	type
L<===>(α′Al) +(Zn)	67.0	381	Eutectic
(α′Al) <===>(αAl) +(Zn)	16.5	277	Eutectoid
(Al) <===>(αAl) + (α′Al)	39.5	351.5	Critical
L<===>Al	0	660. 452	Congruent
L<===>Zn	100	419.58	Congruent

2.5.1 Description of 7075 Alloys

During the initial stages of Aluminium alloy development, the Al-Zn system was considered promising. High temperatures allowed for a significant solubility of zinc in Aluminium, Although this solubility was reduced to 2% at room temperature. Thus, this system was expected to have effective age-strengthening capabilities. Despite that, the resulting hardening was limited primarily due to the formation of deposits of pure zinc. To enhance the age-hardening process, the addition of a small amount of magnesium proved advantageous, as demonstrated by Polmear et al[28]. Magnesium causes noticeable modifications of the hardening phases, of Figure (2.3 a). It is worth noting that the preferential interaction between the relatively smaller zinc atoms and the larger magnesium atoms on the Aluminium lattice played an active role in the decomposition processes during ageing, including certain aggregation mechanisms that cause a reduction in the strain energy of the lattice.

2.5.2 The 7075 Al Alloy System

Intensive research has been carried out on the area that is rich in Aluminium metal in the Al-Zn-Mg three-phase scheme. An example of an isothermal section at a temperature of 200°C is presented in Figure (2.3a). The dissolution and precipitation modelling of the MgZn2-phase, which is of significant interest, exhibited significant variations, particularly at lower and moderate temperatures (T < 300°C). The second figure (2.3b) depicts a recently constructed phase diagram that illustrates the extent to which zinc and magnesium can dissolve in the solid solution of Aluminium. This diagram has been developed using a wide range of experimental data for accurate calibration[29, 30].

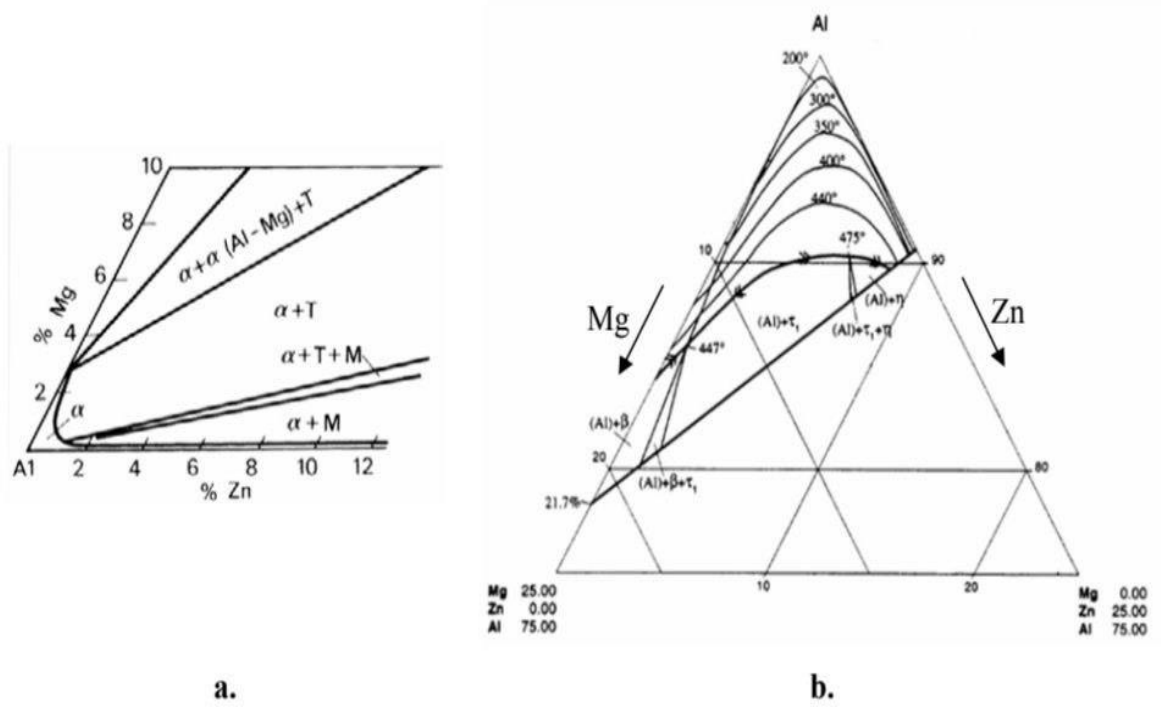

Figure (2.3)**:** In the Al-rich Region, the Phase Diagram of the(Al-Zn-Mg) Alloy Ternary System can be Described; a. Section at 200C^{o} (M=η=MgZn2; T=Al2Mg3Zn3); b. Solvus at Various Temperatures (in at%) [30]

2.6 Heat treatment of 7075 Al Alloys

Heat treatment plays a crucial role in the manufacturing process of engineering components, as it aims to enhance the structural and physical properties of the metal to better align with specific application requirements. Solution heat treatment is a technique employed in Aluminium alloys to facilitate the dissolution of the highest possible amount of a strengthening element into the solution. This is accomplished by subjecting the alloy to a precise temperature, resulting in the formation of a singular phase. The alloy is then held at this temperature for a significant period to ensure complete solution and homogeneity. Rapid quenching follows, preventing the solute atoms from precipitating out of the solution[31]. As a result, the Aluminium matrix forms a highly concentrated solution where solute atoms are spread throughout. The alloy's strength is enhanced through the generation of finely scattered precipitates during the ageing heat treatment, which can occur naturally or artificially. To achieve this, the ageing procedure must be conducted at temperatures lower than the solute equilibrium temperature and beneath a metastable miscibility gap known as the Guinier-Preston (GP) zone solute line[32]. The heat-treatable Al-Zn-Mg (7xxx series) alloy demonstrates a positive reaction to ageing when given sufficient time and suitable temperature conditions for the creation of the stable η phase and its early stages. These alloys offer advantages in industrial settings due to effective strengthening through precipitation, involving the complex breakdown of both stable and unstable phases[31]. In the system consisting of Aluminium, zinc, and magnesium (Al-Zn-Mg system), the presence of larger magnesium atoms on the Aluminium structure, along with clustering to minimize strain energy in the lattice, significantly influences the decomposition processes during ageing [32]. The precipitation thermodynamics in 7075

Al alloy by relating to the Aluminium-zinc binary phase diagram in the Aluminium-rich area is shown in Figure (2.4).

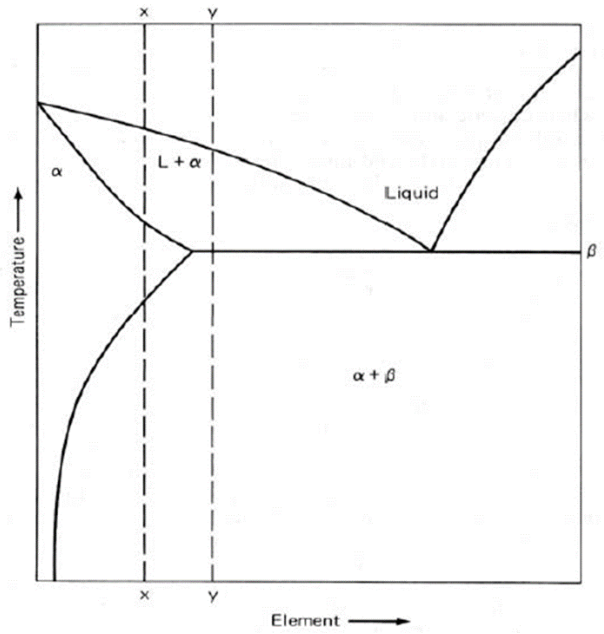

Figure (2.4)**:** Diagram illustrating the schematic process for a hardenable alloy [33]

Solid-solution heat treatment occurs when an Aluminium-zinc alloy with a zinc content of less than 5-6 wt.% is heated just above the solves line. During this process, only one phase remains stable, while the other solid phases dissolve. To achieve the desired results, it is necessary to maintain the specimen at this temperature for an adequate period. Therefore, in order. to subject a sample of 7075 Al (6wt% Zn) to solid-solution heat treatment, the process requires heating the substance to a temperature of 480°C and maintaining it at that level for a duration of 30 minutes. Once the solid-solution sample is rapidly brought below the indicated solvus line shown in Figure (2.3), it experiences swift cooling, leading to the thermodynamic stability of two separate phases, namely, alpha and beta. These phases are physically distinct solids, separated by a phase boundary. The precipitation process involves creating second-

phase embryos through temperature fluctuations and allowing them to develop until they reach a stable state. As time passes, the number of precipitates increases. This progression is known as aging[33, 34]. When the solution attains a balanced composition specified by the solving line corresponding to the ageing temperature, the precipitation stops. For example, at around 380C^{o}, the presence of the Zn-Mg-rich phase in the material causes a decrease in the alpha phase (matrix). The distribution of the precipitates affects the hardness and yield strength, with higher values observed when the precipitates are small and uniformly spread within the matrix, in contrast to larger and scattered precipitates. Thus, to enhance hardness, the specimen needs to undergo heat treatment to generate a finely dispersed and coherent arrangement of small precipitates. [33].

2.7 Mechanical Properties of 7075 Al Alloys

Aluminium alloys containing combinations of magnesium (Mg) and zinc (Zn) belong to a group of heat-treatable alloys. Within this category, some alloys exhibit the highest strengths currently known among commercial Aluminium-based alloys. A key advantage of Al-Zn-Mg alloys, as compared to other Aluminium-based alloys, is their exceptional strength and ductility. This superior performance arises from a unique combination of elements that have significant solid solubility in Aluminium, resulting in the development of remarkably strong precipitate ion-hardening characteristics. However, Al-Zn-Mg alloys demonstrate a robust ageing response due to the breakdown of the over-

saturated solid solution and the formation of finely dispersed Gainer Preston (GP) zones and semi-coherent η' precipitates[35, 36].

Table (2.2) shows some of the mechanical and physical properties of 7075 Al alloy.

Table (2.2)**:** Mechanical Properties of 7075 Al Alloy [37]

7075 AA alloy	
Tensile Strength, MPa	570
Proof Strength, MPa	505
Elongation %	11
Brinell HB	150
Vickers HV	175
Forging temperature C^{o}	350-450
Characterizing	High strength
Applications	Aircraft parts and motor car parts

2.8 Super-plasticity in Alloys

In materials science, superplasticity is a state in which solid crystalline material is deformed well beyond its usual breaking point this may approach 600% during tensile deformation of some advanced materials. Such a state is usually achieved at high homologous temperatures [38]. Superplastic metals possess enhanced malleability, enabling the production of extensive and intricate parts through a singular process, eliminating the need for joints or rivets. This leads to

reduced waste, lower weight, and decreased manufacturing expenses. Additionally, it ensures remarkable precision and eliminates the residual stress commonly associated with welding, making these components exceptionally suitable for aerospace, automotive, and various other applications[39].

2.8.1 Factors Influencing the Super-plastic Behavior of the Alloy

Superplastic materials can be categorized into two main groups: Fine-Structure Superplasticity (FSS), which relates to the internal structural characteristics of the material, such as a stable ultra-fine grain size; and Internal-Stress Superplasticity (ISS), which occurs due to specific external conditions like thermal or pressure cycling. These external conditions induce internal structural transformations, leading to high internal stresses that are independent of external stresses. In both groups, the applied stress required for superplastic deformation significantly depends on the rate at which the material is strained. This relationship is depicted in Figure (2.5). The strain rate sensitivity index provides the most efficient means of evaluating this dependence, denoted as $\boldsymbol{m}$, which represents the strain sensitivity [40].

$$\sigma = C\,(\varepsilon\cdot)^{m} \quad \text{..... (2.1)}$$

$$m\ \left(= \frac{\partial \log \sigma}{\partial \log \varepsilon\cdot}\right) \quad \text{..... (2.2) [42].}$$

where $\boldsymbol{\sigma}$ is the applied stress(N/m^2), The strain rate ($\boldsymbol{\varepsilon}$·) represents the rate of strain in units per second, while (C) MPa is a constant specific to the testing conditions. It is important to know that the constant (C) and the strain-rate sensitivity index are influenced by factors like temperature and grain size, which vary during testing. The strain sensitivity index is typically not higher than approximately 0.8 for superplastic materials. In a tensile test, when $\boldsymbol{m}$ is equal to or greater than $\mathbf{0.5}$, the deformation is expected to be relatively stable. In practical terms, this observation holds, as superplastic materials exhibit increased resistance to necking and achieve high elongations when $\boldsymbol{m}$ exceeds approximately 0.3[42].

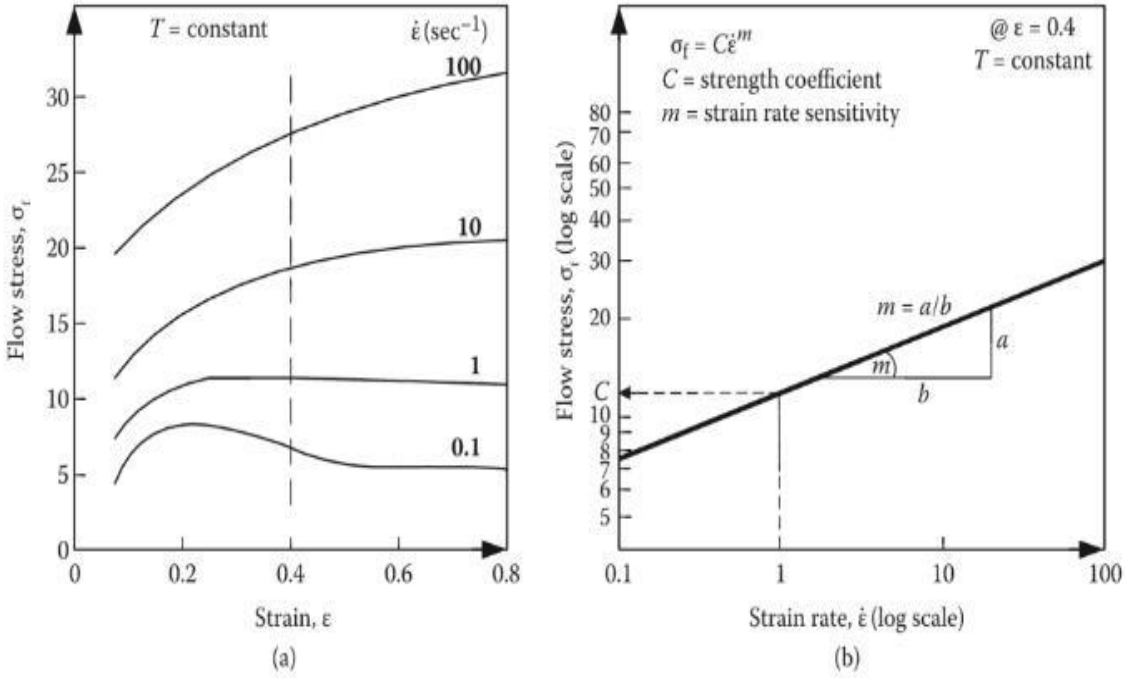

Figure (2.5)**:** (a) Typical Flow Stress-strain Curves at Different Strain Rates

(b). The plot of Flow Stress Versus Strain Rate on a Log-log Scale [41]

The typical ranges of $\boldsymbol{m}$ for different forming conditions are shown in Table (2.3) [41].

Table (2.3)**:** Range of strain-rate sensitivity ($\boldsymbol{m}$) in general to metals

Forming condition	$\boldsymbol{m}$ **range**
Cold forming	$\mathbf{0} < \boldsymbol{m} < \mathbf{0.05}$
Hot forming	$\mathbf{0.05} < \boldsymbol{m} < \mathbf{0.4}$
Superplastic forming	$\mathbf{0.3} < \boldsymbol{m} < \mathbf{0.85}$

2.8.2 Modes for Super Plasticity

There are two modes for Superplasticity: The first is grain boundary sliding (GBS) which is a material deformation mechanism where grains slide against each other as shown in Figure (2.6). This occurs in polycrystalline material under external stress at high homologous temperature (above ~0.4 Tm) and low strain rate [43].

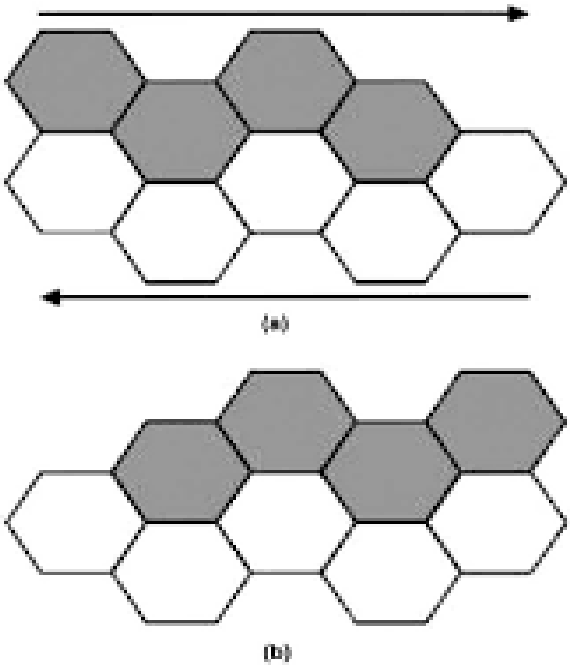

Figure (2.6). Grain Boundary Sliding Model**:** (a) Initial Position of Grains and (b) Position after Top Layer has Slid to Right [44]

The second is the recovery and dynamic recrystallization. Recovery is a superplastic deformation mechanism in which the material undergoes plastic deformation without changing its microstructure. It is a thermally activated process that involves the movement of dislocations within the crystal lattice of the material. This results in the elimination of the strain energy. Recovery is a self-healing process that can occur even at room temperature but is more pronounced at elevated temperatures[45, 46]. Dynamic recrystallization is a superplastic deformation mechanism in which the material undergoes plastic deformation and changes its microstructure through the formation of new grains. Dynamic recrystallization occurs when the strain rate is high enough to generate significant heat, which promotes the formation of new grains. The new grains have a lower dislocation density, which makes them more ductile and allows for further deformation. Dynamic recrystallization is more common at higher temperatures and is often observed in materials such as metals and alloys [47, 48]. Both recovery and dynamic recrystallization are important mechanisms for achieving superplasticity in materials. The choice of the mechanism depends on the material properties, processing conditions, and desired performance characteristics [49].

2.9 Grain Refinement by Plastic Deformation

Grain refinement is a common industrial practice to achieve the formation of small equiaxed grains in the as-cast structure, two approaches can be taken: increasing the quantity of locations where nucleation occurs or promoting grain multiplication. The significance of grain purification in influencing the characteristics of metals and alloys

is widely recognized. This involves enhancing strength, achieving a more refined and evenly distributed porosity, and reducing the likelihood of chemical segregation within the casting. When a material is plastically deformed, the constituent grains of the material are compressed and elongated in the direction of deformation. This deformation causes the formation of dislocations within the grains, which can increase the energy required for grain growth and result in smaller grain sizes. The degree of grain refinement that can be achieved by plastic deformation depends on several variables, including the type of material, the amount of deformation, the deformation rate, and the temperature [50]. In general, materials that are more ductile and have a higher deformation capacity can be more easily refined by plastic deformation. Several grain refinement techniques can be used for metals and alloys, some of which include:

- Mechanical Milling: This process involves ball milling or high-energy milling to produce Nanocrystalline or ultrafine grains in metals and alloys[51].

- Phase Transformation**:** This technique involves inducing phase transformation through rapid solidification or severe deformation to refine the grain structure [52].

- Additives**:** The addition of certain elements or compounds can also promote grain refinement in metals and alloys. For example, the addition of Aluminium or titanium to steel can help in grain refinement.

- Rapid solidification**:** Rapid solidification refers to the process of rapidly cooling a molten metal or alloy at extremely high speeds, resulting in the formation of a solid material with a significantly fine-grained structure. [53].

- Friction Stir Processing (FSP)**:** In this technique, a rotating tool is used to stir the material at high speeds, resulting in a deformation that refines the grains.

- Equal Channel Angular Rolling (ECAR)**:** This technique involves applying high strain rates through a combination of rolling and shearing to produce ultrafine grains in metals and alloys.

-Laser Shock Peening (LSP)**:** This process involves using high-intensity laser pulses to induce shock waves in the material, which can lead to grain refinement [54].

Severe plastic deformation (SPD)**:** One common technique for grain refinement by plastic deformation is severe plastic deformation (SPD), which involves subjecting the material to high strains. Several methods employed in severe plastic deformation (SPD) include equal channel angular pressing (ECAP), high-pressure torsion (HPT), and accumulative roll bonding (ARB). These techniques can be used to refine the grain size of a wide range of materials available, encompassing metals, alloys, ceramics, and polymers. The objective of SPD is to increase the hardness, strength, and ductility of materials[55].

By reducing the grain size, the materials become stronger and harder, while maintaining their ductility. This is because the smaller grain size increases the amount of grain boundaries, which act as obstacles to the movement of dislocations, resulting in an enhancement of strength. The deformation mechanisms during SPD can vary depending on the processing parameters but typically involve a combination of grain refinement, dislocation accumulation, and/or twinning[55]. The resulting ultrafine-grained (UFG) have unique properties due to their increased surface area-to-volume ratio, high density of defects, and altered grain

boundary structure[56, 57]. Presently, there is a significant scientific fascination with ultrafine-grained materials because of their significant mechanical and physical characteristics. These materials exhibit enhanced stress life, and heightened damage tolerance, and are attainable through various methods. Methods such as rolling, extrusion, pressing, or hammering, collectively known as extreme deformation of plastics (SPD), enable the achievement of exceptionally high strains in the material. However, it is important to note that this process often leads to noticeable changes in the material's dimensions. By studying the mechanisms behind extreme deformation in plastics, engineers can improve process designs and enhance the accuracy of predicting process outcomes[58]. Overall, The enhancement of material characteristics through the process of plastic deformation shows great potential as a method to refine the grain structure and has potential applications in industries used in the production of metals for high-performance applications including aerospace, automotive, and biomedical industries. For instance, SPD can be used to improve the mechanical properties of structural materials such as Aluminium alloys, magnesium alloys, and titanium alloys where materials with high strength and fatigue resistance are required. It can also be used to fabricate biomedical implants with improved biocompatibility, corrosion resistance, and mechanical properties [59].

2.10 Machinability of Al-base alloy

Using lightweight materials is an effective strategy to decrease the weight of structures. Aluminium alloys are widely utilized as lightweight metals due to their diverse mechanical and thermal properties. Moreover,

metals, particularly Aluminium alloys, are easily malleable, especially during processes like machining. In comparison to other lightweight metals such as titanium and magnesium alloys, Aluminium alloys are considered to be highly machinable. This characteristic plays a crucial role in determining processing performance and can be tailored for specific applications based on parameters such as the longevity of the tool, the quality of the surface produced, the ability to remove chips effectively, the rate at which material is removed, and the power required by the machine tool are all influenced by various aspects. The chemical composition, structural imperfections, and presence of alloying elements have been demonstrated to exert a noteworthy influence on the machinability of these materials[60]. Therefore, by employing various treatments, the machinability of alloys can be enhanced, given their similar chemical compositions. Heat treatments, which increase the hardness of alloys, can decrease the occurrence of built-up edge (BUE) during machining [61]. When dry machining is involved, certain problems arise in particular situations, for instance, (BUE) when cutting speeds are slow, and another issue known as sticking when cutting speeds are high, necessitating the utilization of specialized tool geometries. Studies have shown that higher levels of Magnesium (Mg) cause cutting forces to rise even when the hardness remains constant [62]. Reducing the amount of Copper (Cu) in Aluminium alloy 319 reduces the cutting force. As for the impact of heat treatment on 6061 alloys, specifically the ageing process, it only affects the forces at low cutting speeds. This is because the temperature increase in the cutting area is minimal at high speeds, leading to a negligible influence[63]. The consensus is that the majority of Aluminium alloys that have been worked on show remarkable ease of machining. On the other hand, Machining may become challenging when working with cast alloys that

contain copper, magnesium, or zinc as the primary alloying elements. However, employing small tool rake angles can help alleviate this issue. Silicon-containing alloys, on the other hand, Require bigger tool rake angles, reduced speeds, and feeds, which makes them more economically viable for machining. Unlike Aluminium alloys that cannot undergo heat treatments, they can be hardened through cold work, resulting in improved machinability when using sharp tools[64].

2.10.1 Variables Affecting the Machining Properties of 7075 Al Alloy

Aluminium is a material that can be machined with ease, although using softer grades may result in lower-quality surface finishes due to the formation of a build-up edge. To address this concern, it is recommended to employ high cutting speeds, high rake angles, and high relief angles. Achieving precise dimensional tolerances when machining Aluminium can be challenging, mainly because of its high thermal expansion coefficient and relatively low elastic modulus. In comparison to ferrous alloys, machining Aluminium alloys typically requires significantly less cutting force. This is because Aluminium alloys have lower mechanical strength, resulting in cutting pressures that are approximately 70% lower than those needed for machining steels[64]. Nevertheless, it should be emphasized that this variance is relatively insignificant when comparing different types of Aluminium alloys, as it is affected by their chemical composition and physical characteristics [65, 66]. Applying thermal or mechanical treatments to Aluminium alloys, or introducing chemical elements that enhance their hardness and mechanical strength, can

decrease the area of contact between the chip and the tool, potentially resulting in reduced machining forces[67]. The 7075 Aluminium alloy, which is frequently utilized in aerospace and other demanding situations, is known for its exceptional strength. It is also known for its excellent machinability, although it can be more difficult to machine than some other Aluminium alloys due to its high strength [68]. The mechanical machinability of 7075 Aluminium alloy can be enhanced by using appropriate machining parameters. Additionally, the use of high-performance cutting tools made of carbide or diamond can help improve the machining process. It is important to note that machining 7075 Aluminium alloy can generate a large amount of heat, which can cause the material to become distorted or even crack. Therefore, proper cooling and lubrication are essential to prevent heat buildup and maintain the quality of the machined parts [69].

2.10.2 Determining the Machinability of the Metallic Alloys

There are several factors used to evaluate the machinability of materials, The following are the most frequently utilized factors: the lifespan of the tool, which affects the time and costs involved in machining; the forces applied during cutting, which impact energy usage; the temperatures generated during cutting, which affect the wear and tear of the tool; the quality of the surface being machined; and the shape of the chips produced. Considering these factors allows for the achievement of enhanced material machinability through prolonging the lifespan of tools, increasing productivity by facilitating greater chip removal, improving surface quality, reducing cutting forces, minimizing cutting temperatures, and obtaining more desirable chip shapes.

However, it is crucial to ensure that these improvements are attained under the same conditions. When machining different materials under consistent conditions, variations in cutting forces emerge due to the distinctive physical and chemical properties of the workpiece material. The primary cutting force is influenced by material properties such as tensile strength and hardness. Additionally, various factors, including microstructure, crystal grain size and shape, type and quantity of impurities, and additional elements, also affect the primary cutting force. Thus, it is essential to consider these aspects [67]. Surface roughness plays a crucial role in the surface topography and mechanical properties of a part, such as fatigue life and tensile strength. In addition to influencing the properties and functionality of machined components, surface roughness is a significant parameter for dimensional accuracy. Three factors that affect surface roughness in any part or component are geometric factors, machine tool factors, and the material of the workpiece. Machining conditions also contribute to the surface roughness[70].

2.11 literature Review

Kannan and Ramanujam in 2017 [71] The study examined Aluminium-based nanocomposites, comparing single-reinforced and hybrid reinforced materials. Single reinforced nanocomposites used AA 7075 Aluminium alloy combined with 2 wt.% 30-50nm nano alumina particles. Hybrid reinforced nanocomposites included 4 wt.% silicon carbide (5-10μm) and either 2 wt.% or 4 wt.% nano alumina particles. Single reinforced nanocomposites were produced by stirring and casting at temperatures of 400^0C, 500^0C, and 600^0C, while two hybrid

reinforced nanocomposites were created at 500^0C. A single reinforced nanocomposite was also generated through squeeze casting at 101 MPa.

Agarwal et al. in 2019 [72] aimed to examine the manufacturing process and assess the machinability of a hybrid nanocomposite named squeeze cast AA 7075/h-BN/Graphene. The formation of this composite involved combining hexagonal boron nitride (hBN) and graphene nanoparticles (GNPs) in precise weight ratios (0.5% h-BN and 1% GNPs). It was essential to ensure a uniform blend of these nanoparticles to make optimal use of their self-lubricating characteristics. Thus, before squeeze casting the hybrid nanocomposite, a technique called ball milling (BM) was employed to ensure uniform mixing and prevent nanoparticle agglomeration. The investigation utilized scanning electron microscopy (SEM) and optical microscopy (OM) to confirm the even distribution of nanoparticles and a reduction in grain size.

Haydar Al-Ethari et al. in 2020 [73] examined how mechanical and thermo-mechanical treatments affect the microstructure and hardness of an Al5Zn1.8Mg alloy. The alloy samples were prepared by casting, with mechanical mould vibration applied at a frequency of 25Hz and an amplitude of 0.5mm. Thermo mechanical treatment involved warm shaping after precipitation and age hardening at a temperature of 200°C, using forming pressures of 200, 300, and 400MPa.

Österreicher et al. in 2020 [74] introduced an economic procedure for shaping automotive components using pre-aged AA7075 sheets at temperatures ranging from 180 to 250 °C. This method offers a balance between easy shaping and enhanced paint-baking characteristics. The resulting parts exhibit approximately 95% of the maximum strength of

peak-aged AA7075. The precipitation that occurs during the manufacturing process was analyzed using differential scanning calorimetry and transmission electron microscopy.

Hua et al. in 2020 [75] focused on investigating the changes in the internal structure of AA7075 Aluminium alloy after annealing and how it affected its ability to deform at room temperature. Various annealing experiments were carried out using different temperatures and durations.

Soni and Thomas in 2020 [76] focused on analyzing the microscopic composition, physical properties, and ease of machining of a unique combination of squeeze-cast AA7075 and AA7075/SiC/h-BN nanocomposite. By introducing micro-sized SiC particles (1 wt.%) and h-BN nanoparticles (0.5 wt.%) into the AA7075 alloy, its strength was enhanced. These additions were incorporated into the alloy through an ultrasonic-assisted melt-stirring technique. To ensure better reinforcement mixing, prevent nanoparticle agglomeration, and improve the wetting of particles in the molten state, the SiC and h-BN powders underwent ball milling for a duration of 4 hours.

Rajesh et. al in 2021[77] focused on investigating the mechanical properties of composite materials made from a blend of Al 7075 alloy, fly ash, and silicon carbide (SiC) using the stir cast technique. The research examined how the inclusion of fly ash and SiC strengthened the AA7075 compound. Different weight percentages of fly ash and SiC were mixed with the metal matrix materials, ranging from 0 to 10 per cent. The prepared materials were then evaluated using equipment to measure tensile strength and hardness. The incorporation of fly ash resulted in increased hardness and improved tensile attributes, such as

ultimate stress and yield stress, when SiC grains were added. The study also addressed methods to enhance these properties further.

Wang et al. in 2022 [78] investigated how semi-solid AA7075 Aluminium alloy deforms using the direct partial re-melting method with as-extruded billets. The study revealed that both inter-granular and intra-granular deformation take place concurrently when compressing the alloy under semi-solid conditions. The deformation of solid primary grains helps offset the shrinkage of the liquid between the grains, ultimately enhancing the overall integrity of the formed components. Additionally, the intra-granular deformation that occurs towards the end of the semi-solid processing leads to alterations in the shape of the spherical solid grains and the formation of sub-grain boundaries.

Parakh et al. in 2022 [79] investigated the AA7075 alloy under different pressure conditions using diamond anvil cells. The pressures reached approximately 53 GPa. To examine the changes in the alloy's microstructure and estimate its strength under high pressure, researchers employed in situ X-ray diffraction (XRD) and transmission electron microscopy (TEM) imaging techniques before and after applying compression.

2.12 Summary of the Literature Reviews:

Table (2.12) summarizes literature related to the 7075 Aluminium alloy produced by stir casting.

No.	Authors	Alloy	Objective	Ref.
1.	**Kannan and Ramanujam**	AA7075 alloy	The mechanical and alloy microstructural	[71]
2.	**Agarwal et al.**	AA 7075/h-BN /Graphene (HNC)	The fabrication and the machinability of the alloy.	[72]
3.	**Haydar Al-Ethari et al.**	AA7075 alloy	The influence of mechanical mould vibration, as well as its frequency, on the outcome.	[73]
4.	**Österreicher et al.**	AA7075 alloy	Precipitation during the production process was studied.	[74]
5.	**Hua et al.**	AA7075 alloy	The microstructure of the annealed alloy.	[75]
6.	**Soni and Thomas**	AA 7075 andAl7075/SiC/h-BN	The mechanical properties and machinability of alloys	[76]
7.	**Rajesh et. al**	AA 7075 alloy	The fly ash and SiC enhance the mechanical characteristics of the Al 7075 alloy.	[77]
8.	**Wang et al.**	AA 7075 alloy	The deformation mechanisms 7075 alloy	[78]

9.	**Parakh et al.**	AA 7075 alloy	The response of Al7075 alloy to semi-hydrostatic and non-hydrostatic pressure	[79]

The objective of the study is to enhance the machinability of 7075 Aluminium alloys by implementing a warm squeezing technique on the alloy. The focus is on investigating the impact of grain structure and distribution, which aids in reducing pores and modifying the alloy's structure. This involves the fragmentation and refinement of the alloy's grains, resulting in reduced grain size and improved homogeneity. By achieving a uniform distribution of grains, the microstructure becomes more homogeneous, leading to enhanced mechanical properties such as hardness, elasticity, tensile strength, and machinability. These improvements are attributed to grain smoothing, gap removal, and increased homogeneity.

Chapter Three

Chapter Three

The Experimental Work

3.1 Introduction

This chapter presents an overview of the materials and equipment used in the study. The experimental work used to prepare the samples and the processes used in this study will be clarified. Also, the mechanical, physical and chemical tests used will be reviewed in this chapter to provide readers with a clear understanding of the experimental methodology and ensure the validity of the findings in the work.

3.2 Program of the Current Study

The plan of the current Study and the method utilized to prepare the samples and all the tests are shown in Figure (3.1).

3.3 Materials and Samples Preparation

To achieve the goal of the current study, the materials used to prepare the samples and their specifications are shown in Table (3.1).

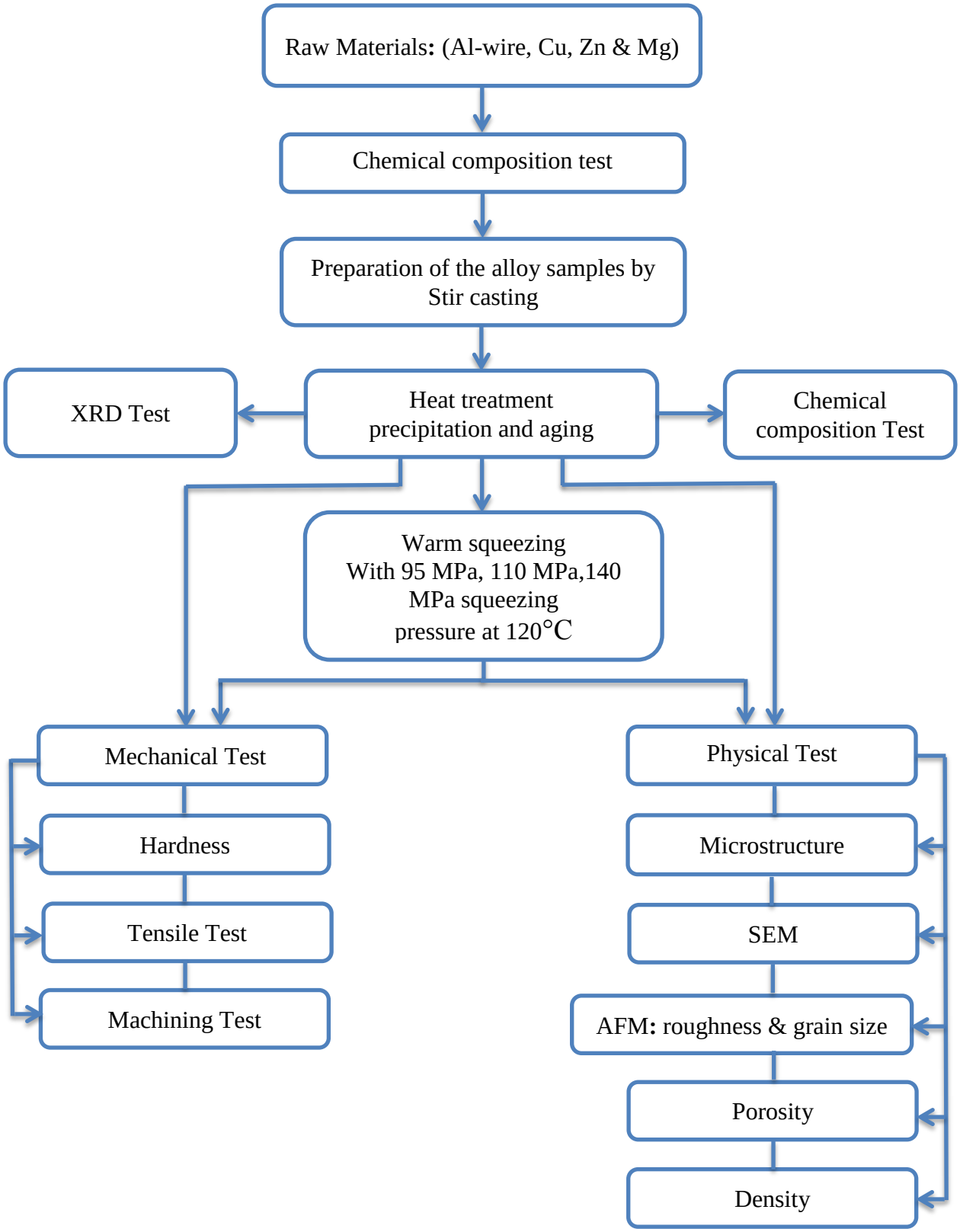

Figure (3.1): Experimental Program of the Present Study

Table (3.1)**:** Materials used in the current study

material	Chemical Composition or Source								
Aluminum Wires (%)	Al Wt. %	Fe Wt.%	Mg Wt.%	Si Wt.%	Zn Wt.%	Ti Wt.%	Cr Wt.%	Cu Wt.%	Other Elements Wt.%
	99.7	0.113	0.1201	0.022	0.02	0.004	0.003	0.001	0.0169
zinc	-Small solid pieces with 99.9% purity BHD Chemical Ltd Poole England USA. Oxford LABORATORY REAGENT (iso:9001-2008)								
Magnesium	-Mg ribbon roll of 99.8% purity Magnesium ribbon roll, each role is (25g) in weight. Pure Magnesium Tape for Science & Lab Tape Rolls, by American Heritage Industries								
Copper	-Powder of 99% purity USA. Oxford LABORATORY REAGENT (iso:9001-2008)								

3.4 Preparation of the Alloy Samples

Pieces of aluminium wire were melted in a ceramic crucible via a gas furnace at 670°C in an inert gas atmosphere. The temperature was controlled using an infrared camera type (AR-882 smart sensor). The molluscs were removed using an alumina spatula. Copper, zinc and magnesium due to the required ratio were wrapped separately with aluminum foil and gradually added to the melt. The melt was stirred manually by a ceramic rod for 15 minutes. The melt was poured onto a steel mould preheated to 300 °C with cylindrical cavities with a diameter of 15 mm and a height of 165 mm as shown in Figure (3.2).

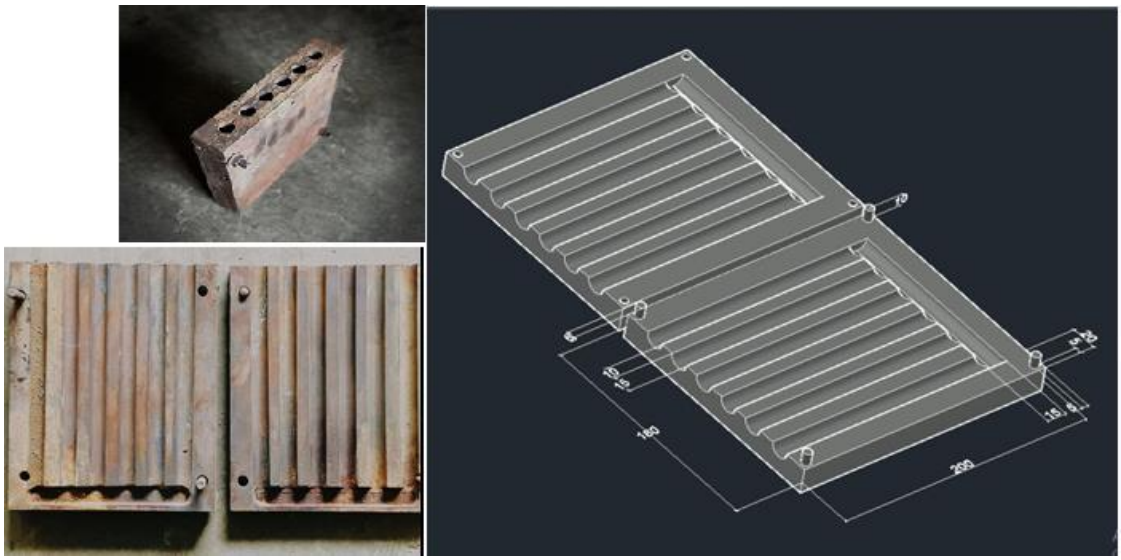

Figure (3.2)**:** The Steel Mold Used to Prepare the Alloy Samples

The cast samples were homogenized at 520°C for 4 hours in an electric furnace type (B. Lindberg solar basics). The homogenizer samples were left to cool inside the furnace. Precipitation and age-hardening heat treatment for the cast samples was carried out via a furnace type (Sola Basic SB Lindberg). The samples were heated to 480°C with a heating rate of 10°C/min, maintained at this temperature for 30 min, then quenched in iced water. Then the samples were heated at 120°C for 5 hours and cooled slowly inside the furnace.

A chemical composition analysis for the prepared samples was carried out.

3.5 Warm Squeezing of the Samples

Warm squeezing was carried out to improve some properties of the cast alloy samples. Specimen of the cast samples was subjected to several squeezing pressures of 95MPa, 110MPa, and 140MPa at 120°C for a duration time of 10 minutes. The squeezing pressure was defined due to many trials to obtain the best results, and one pressure was determined,

which was 140. A cylindrical specimen with 15 mm - diameter and 165 mm - length was fitted in a cylindrical steel die having an internal diameter of 15 mm and then subjected to axial squeezing load. The squeezing process was performed via an electric press type (CARVER). A specifically crafted and constructed apparatus, depicted in Figure (3.3), was utilized to carry out the heating procedure. Figure (3.4) shows the steel die used to perform the squeezing process.

Figure (3.3)**:** (a) The Controller of Temperature; (b) Press Type (Carver) Used to Perform the Squeezing of the Samples; (c) The Designed Heating Element

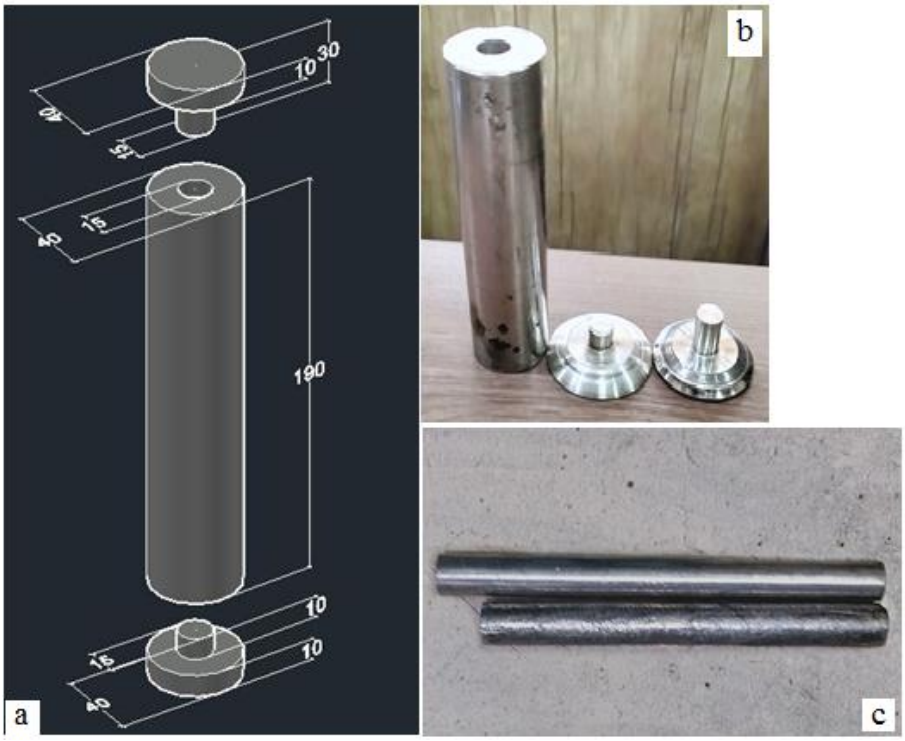

Figure (3.4)**:** (a) Geometric Drawing of the Die Used for Squeezing the Sample; (b) The Die Used to Perform Squeezing of the Sample; (c) Sample before and after Squeezing

3.7 Physical Test

3.7.1 Microscopic Analysis

All specimens were properly cleaned and ground using silicon carbide grinding papers (180, 400, 600, 800, 1000, 1200, 2000, 2500, and 3000 coarseness measures), and the MP-2B grinder polisher was used for both grinding and polishing operations. Polishing and cleaning were done using diamond sheets a 0.2 mm jewel arrangement. Thereafter, For 12 seconds at room temperature, a solution of Keller's reagent was administered. the presented solution consisted of 95 millilitres of water, 2.5 millilitres of nitric acid, 1.5 millilitres of hydrochloric acid, and 1.0 millilitres of hydrofluoric acid [80]. The specimens were then rinsed with

distilled water and dried using an electric drier. The test was conducted via a BEL PHOTONICS-type microscope provided with a digital camera to capture the microstructure. This test was conducted in the sample preparation laboratory at the College of Materials Engineering / University of Babylon / Iraq

3.7.2 Scanning Electron Microscopy (SEM) Test.

In the present work, SEM is used to reveal the microstructure to characterize the surface shape and properties of the samples. The examination was performed by a scanning electron microscope type (VEGA3SBU) shown in Figure (3.5). The samples were prepared following the same guidelines used for the optical microscopic test. This test was conducted in the laboratory complex of the Department of Ceramic Engineering/College of Materials Engineering / University of Babylon / Iraq

Figure (3.5)**:** A scanning electron microscope (VEGA3SBU).

3.7.3 X-Ray Diffraction Test

X-ray diffraction analysis (XRD) is a method used to ascertain Crystal arrangement and phase composition in materials. In the case of aluminium alloy 7075, XRD analysis can be used to determine the different phases present in the alloy and their relative proportions.

A sample of 7075 aluminium alloy has been prepared by cutting or grinding it into a small, flat, and smooth surface. The sample shall be free of any impurities or surface defects.

An appropriate X-ray emitter, such as a source of copper (Cu) K-alpha radiation with a specific wavelength, is needed. of 1.5418 Å and a high-resolution X-ray diffractometer was used with a theta angle range (2θ) of 10–80°, and a step size of 0.02°. A diffraction pattern was collected By scanning the sample over 2 degrees.

3.7.4 Atomic Force Microscopy (AFM) Test

Atomic force microscopy (AFM) is a method that may be used to analyze the topography and other characteristics of surfaces. AFM creates enlarged, or three-dimensional, pictures of surfaces with a resolution of a few nanometers by scanning a surface sample. Figure (3.6) shows the AFM (AA3000 Scanning probe microscope) used in the present study. This test was conducted in Polymer Engineering Laboratories/College of Materials Engineering / University of Babylon / Iraq

Figure (3.6)**:** Atomic Force Microscopy Type (AA3000 Scanning Probe Microscope)

3.7.5 Porosity Test

The test was carried out according to ASTM (B 328 - 96), and the following equation was used.

$$\text{porosity} = \frac{Ww - Wd}{Wsat - Ws} \times 100 \quad \ldots \ldots (2.1)$$

The paragraph describes the measurements of different weights in a sample. The dry weight of the sample (Wd) is determined by weighing it after it has been completely dried. The wet weight of the sample (Ww) is measured by weighing it after it has been immersed in distilled water for 24 hours. The saturated weight (Wsat) is obtained by weighing the sample after it has been immersed in water at 80 degrees Celsius for 5 hours. The suspension weight (Ws) refers to the weight of the sample when it is suspended in distilled water.

3.7.6 Density Test

According to the international standard ASTM D-792 [81], density was determined by Archimedes' principle**:** this method involves measuring the displacement of water, as it uses the principle of buoyancy to determine the density of an object. The object is suspended in the water using a wire, and the amount of water displaced is measured. The buoyant force acting on the body is equal to the weight of the displaced water, which is also equal to the weight of the body. By dividing the body's weight by its volume, the density can be determined.

3.8 Mechanical Test

3.8.1 Hardness Test

Hardness tests were performed on three samples representing: Homogenized sample, heat-treated sample, and warm-squeezed sample. Samples measuring 15 mm in diameter and 10 mm in height were fabricated to conduct the Brinell hardness test, following the guidelines outlined in ASTM (E10-15a). shown in Figure (3.7), with a ball diameter of 2.5 mm and a load of (31.25 g) for (10) seconds.

Figure (3.7)**:** Brinell Hardness Device Type (Wilson Hardness, REICHERTER UH 250)

Before testing, appropriate grinding and polishing processes were performed for each sample. Hardness was recorded as an average of three readings. Tests were performed with a type hardness tester (Wilson Hardness, REICHERTER UH 250).

Vickers test has been conducted according to ASTM (E384). The tests were carried out using the hardness tester (HVS-1000) shown in the figure (3.8).three readings.

Figure (3.8)**:** Vickers hardness Device Type (HVS-1000)

3.8.2 Tensile Test

Following ASTM (B557m-15) [82], standard samples were constructed with the dimensions shown in Figure (3.9).

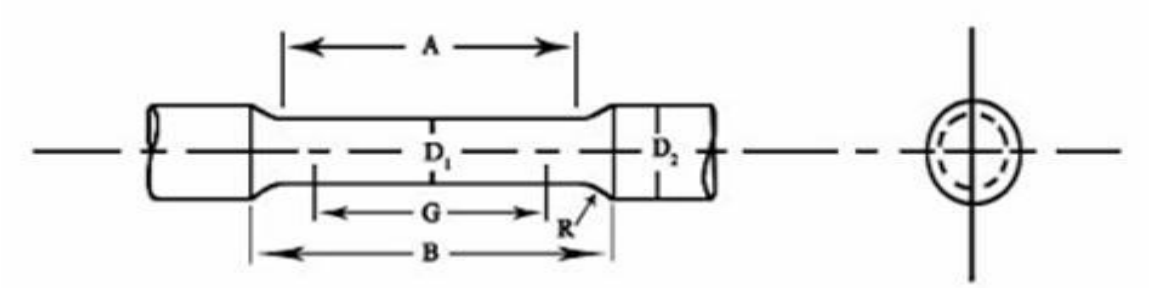

Figure (3.9)**:** Standard Round Tension Test Specimen [82]

Where**:** Radius of Fillet (R)**:** 6 mm; Gage Length (G)**:** 35 mm; Diameter (D)**:** 8.75 mm; Length of Reduced Section (A)**:** 45 mm

The samples were polished to remove any surface defects. The tests were carried out with a speed rate of 0.2 mm/min via a computer-controlled universal testing machine (WDW) model. The tests were performed on two types of samples: heat treated only, and heat treated and warm squeezed. The test was conducted at the ambient temperature and temperatures of 200°C, 250°C and 350°C. A specially designed and built heating system with a heating element and a thermocouple to measure the temperature was used to perform the tests as shown in Figure (3.10).

Once the sample has reached the desired temperature, a tensile test is started slowly on the sample until it reaches the breaking point. The test was carried out at different temperatures to determine the extent to which the thermal tensile strength of the alloy varies with the temperature.

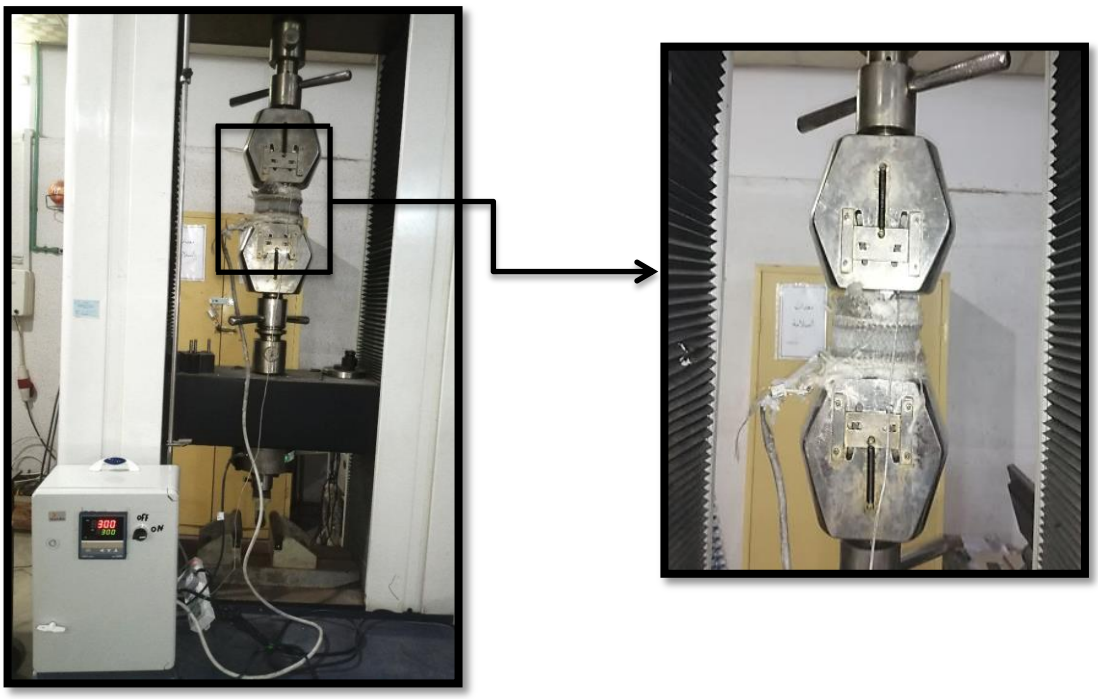

Figure (3.10)**:** Tensile Testing Machine with Heating System

3.8.3 Machining and Machinability of Alloys

The machining tests were conducted on a lathe type ZMM-Sliven/Bulgaria with the specification (2.2 kW motor, spindle speeds in the range of 20-2000 rpm feed rate in the range of 0.015-0.6 mm/rev).

For the curing experiments, P10-type cemented carbide tips were employed. These tips have a chemical composition consisting of 65% tungsten (W), 9% cobalt (Co), and 26% tantalum carbide (TaC) and titanium carbide (TiC) combined. The tips had four cutting edges and were designed with a tool angle of 55° and a nose radius of 1.6 mm. To hold the tool, an AG.CO tool holder type was utilized. The cutting was performed under dry conditions, maintaining a constant cutting depth of 0.2 mm. Three different cutting speeds were employed namely 7 m/min, 14 m/min, and 52 m/min. Additionally, two feed rates were applied during the processing conditions, namely 0.130 mm/rev and 0.70 mm/rev

The machinability of the alloys was explored by measuring the cutting force, the roughness of the machined surface, and the shape and size of the chip. Measuring cutting forces during fabrication can provide valuable insights into the machinability of an ingot. One way to measure this is to calculate the cutting forces required to machine the material. Cutting forces are typically measured in three directions: axial, radial, and transverse. A cutting force dynamometer was used for this device to measure The forces exerted on the cutting tool during machining. Figure (3.11) shows the dynamometer and its arrangement on the lathe.

Figure (3.11)**:** The Dynamometer and Its Amendment on the Lathe

The surface roughness of the machined surface was measured via a roughness tester type (HSR 210 Roughness Tester, China). All measurements were made after the first minute of cutting, which used a probe to touch the surface of the alloy and measure its texture. The maximum reading was taken directly and the average of three readings was recorded for each process.

An image of the chip shape produced by each machining process was captured to provide insight into the deformation behaviour of the alloy during processing.

Chapter Four

Chapter Four

Results & Discussions

4.1 Introduction

In this chapter, the results are presented and discussed under various aspects; effects of warm squeezing of the 7075 Al-alloy on its metallurgical, physical, and mechanical properties and choosing the best pressure and temperature parameters and studying their effect on these properties

4.2 Chemical Composition Analysis:

Table (4.1) shows the results of the chemical composition of The prepared alloy (Al-Zn-Mg). The analysis was carried out at the General Company for Engineering Testing and Qualification/ Baghdad.

The results included (Bal.% of Al- 5.4% of Zn- 2.3 of Mg) in addition to other elements as impurities in this alloy.

Table (4.1) The chemical composition of the prepared alloy.

Element	Zn(%)	Mg(%)	Cu(%)	Mn(%)	Fe(%)	Si(%)	Al(%)
Prepared alloy	5.4	2.3	1.3	0.006	0.4	0.08	Bal
Stranded (%)[83]	5.1-6.1	2.1-2.9	1.2-2	Max. 0.3	Max. 0.5	Max. 0.4	Bal

4.3 Results of the Physical and Mechanical Tests:

4.3.1 Optical Microscope Analysis

Figure (4.1) shows the optical microstructure of the heat-treated and the squeezed samples using microscope magnification (100x). The warm squeezing in all directions leads to a decrease in grain size, and it showed more homogeneity for the thermally squeezed microstructure. In addition, it reduced the porosity.

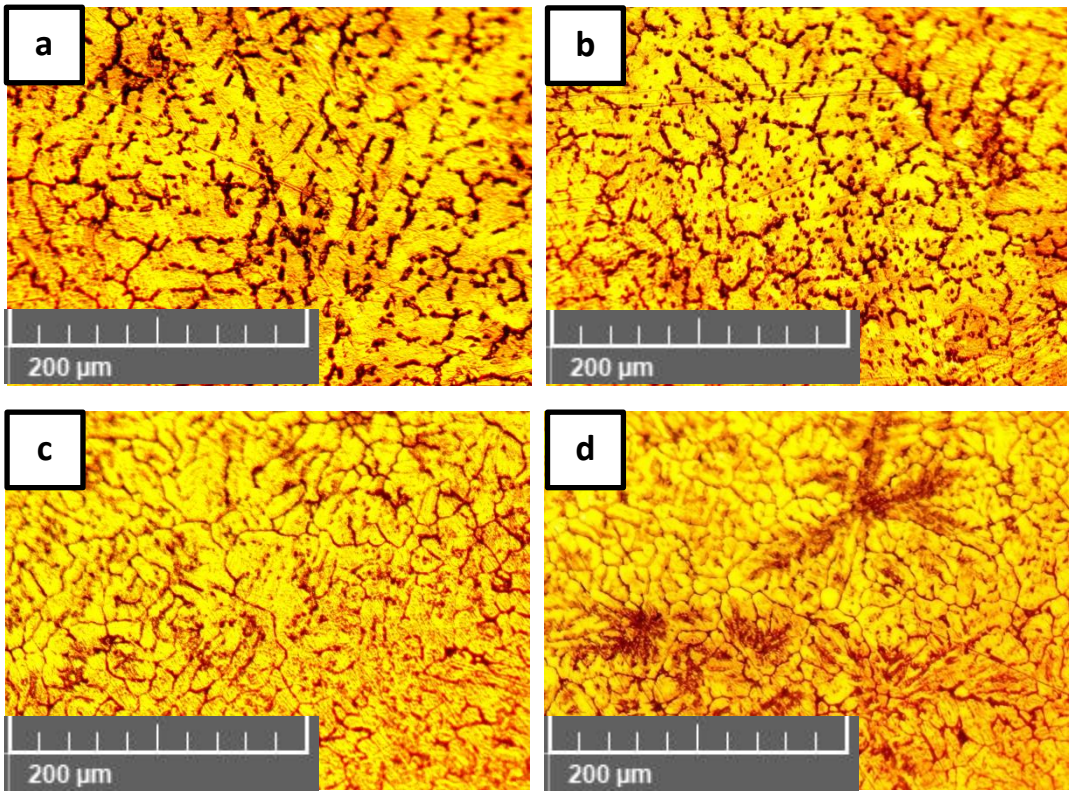

Figure (4.1)**:** Microstructure (100x) (a) Heat-treated before Squeezing; (b) Heat-treated and Squeezed at 95MPa; (c) Heat-treated and Squeezed at 110MPa; (d)) Heat-treated and Squeezed at 140MPa

4.3.2 X-ray Diffraction (XRD) Analyses:

Figure (4.2) shows the XRD analysis of the processed and heat-treated 7075 Al alloy, and the positions of the obtained diffraction Peaks.

Are in agreement with the corresponding values of the phases reported in (4.2) and shown in appendix(1). The phases in the alloy appeared as a result of the heat treatment. These phases are considered one of the strongest phases in 7075 Al alloy and are characterized by hardness and strength. The influence of phases on the qualities of the alloy is especially prominent in strength, elasticity and hardness.

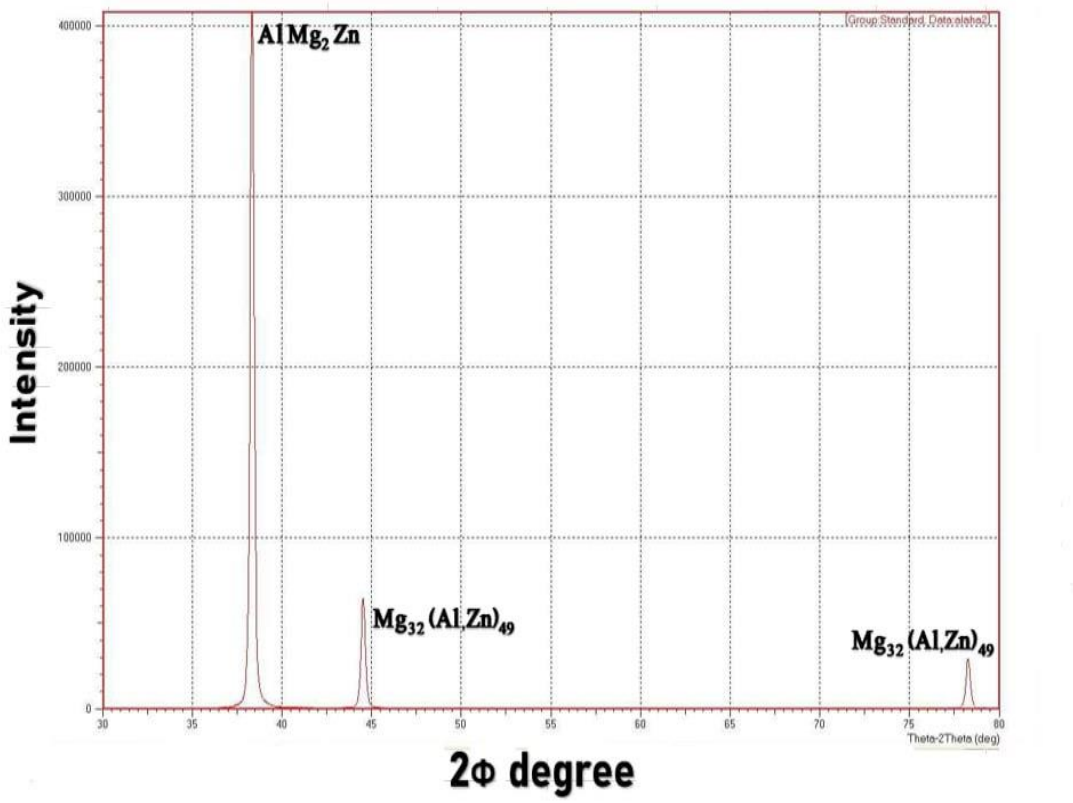

Figure (4.2)**:** XRD Analysis of the Prepared and Heat treated

7075 Al-alloy

4.3.3 Scanning Electron Microscopy (SEM) Analysis:

Figure (4.3) shows the SEM images of the tested samples. The results indicate how significantly the pores and gaps shrank and a more uniform structure was obtained as a result of the warm squeezing applied to the

grains in all directions, as well as how the grain size decreased. The result of deformation compared to grain.

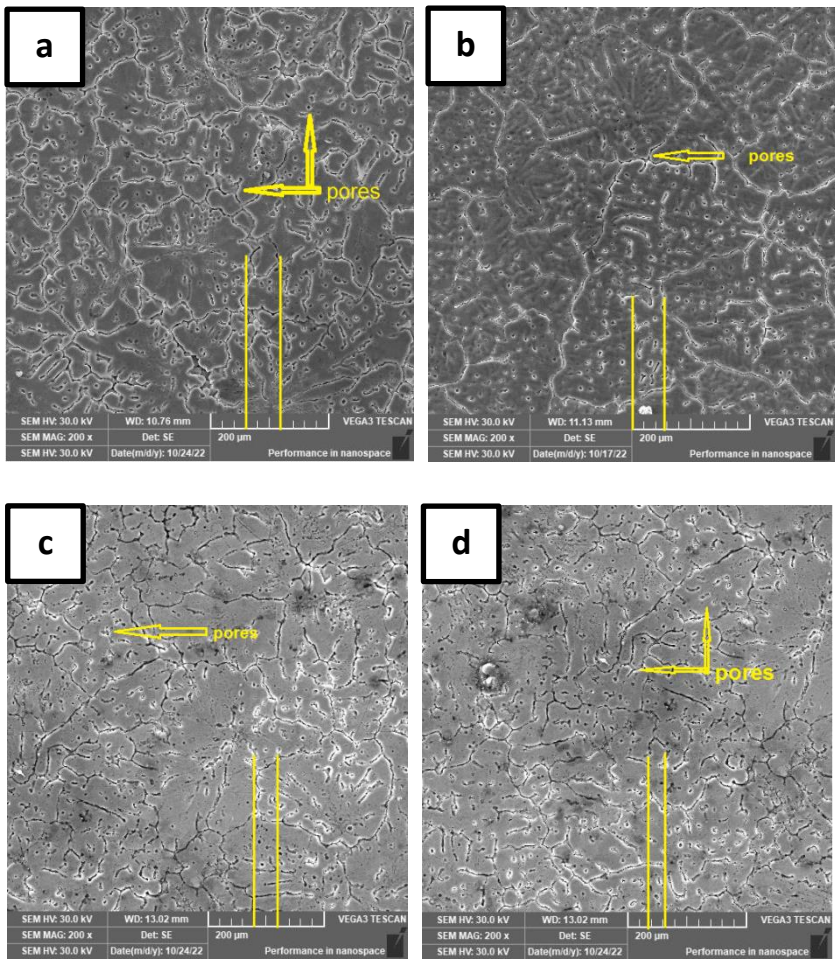

Figure (4.3)**:** SEM image of the Prepared and Heat treated 7075 Al-alloy (a) Heat-treated before Squeezing; (b) Heat-treated and Squeezed at 95MPa; (c) Heat-treated and Squeezed at 110MPa; (d)) Heat-treated and Squeezed at 140MPa

4.3.4 Atomic Force Microscopy (AFM) Analysis:

Figure (4.4) shows three-dimensional images at the nanometer scale by atomic force microscopy. The surface topography of the alloy are

shown before and after warm squeezing. The average nanometer diameter of the sample grains was recorded before and after the squeezing and demonstrated in Table (4.2). Figure (4.4) shows how the surface topography differed after the warm squeezing procedure.

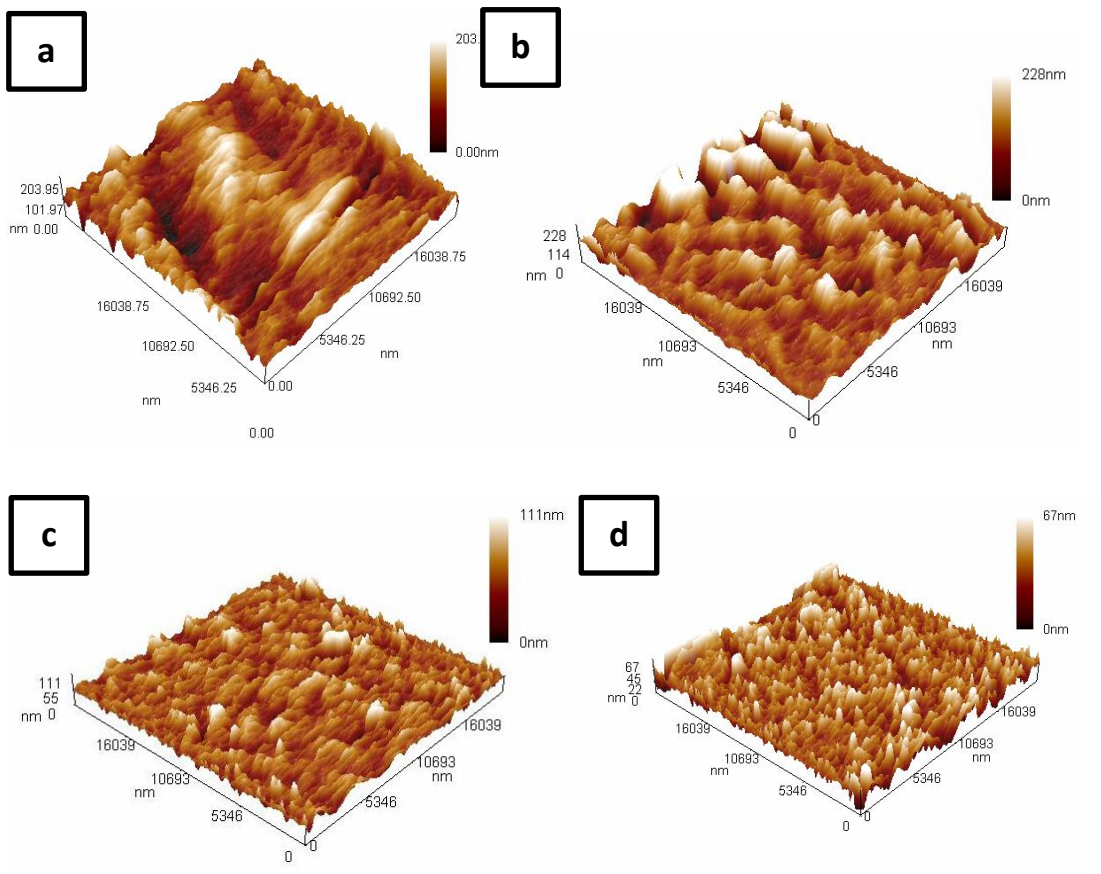

Figure (4.4)**:** 3D atomic Force Microscopy Images of the Prepared and Treated 7075 Al-alloy**:** (a) Heat-treated before Squeezing; (b) Heat-treated and Squeezed at 95MPa; (c) Heat-treated and Squeezed at 110MPa; (d)) Heat-treated and Squeezed at 140MPa

Table (4.2)**:** The Average Granular Diameter of the Samples.

Sample	**Avg. diameter(nm)**
Heat treated before squeezing	962
Heat treated and squeezed by 95**MPa**	737
Heat treated and squeezed by 110**MPa**	702
Heat treated and squeezed by 140**MPa**	655

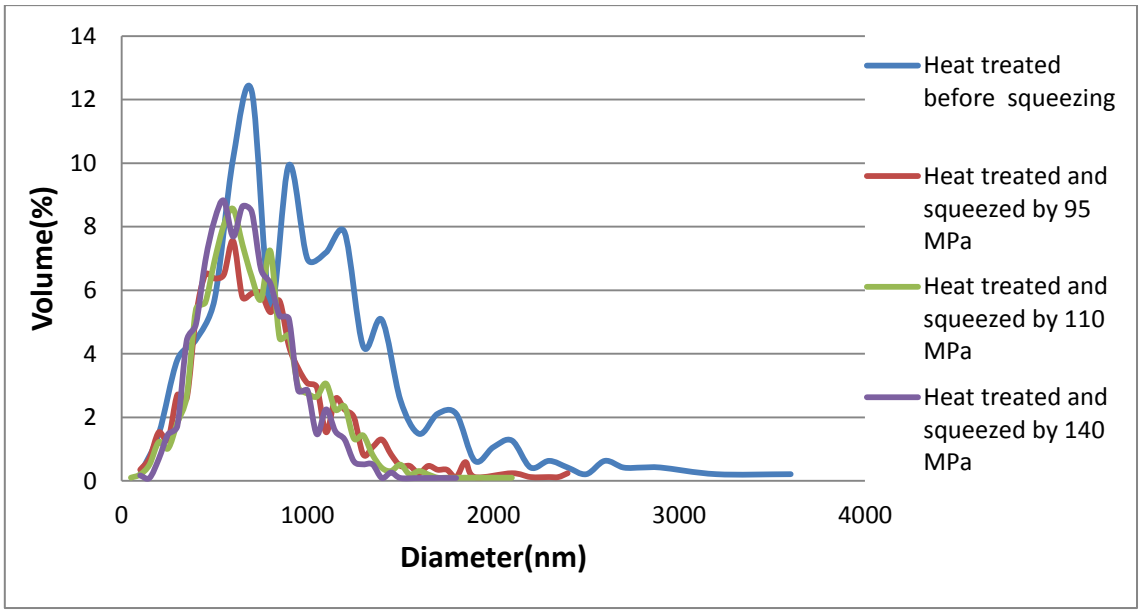

Figure (4.5)**:** Average Grain Diameter of Samples Relative to Size

The results indicate that an increase in the amount of squeezing pressure leads to decrease in the size of the grains. Figure (4.6) shows the size of the grains before the warm squeezing process and after the warm squeezing process, as it shows that an increase in the amount of

three-dimensional warm squeezing leads to a further decrease in the size of the grains and makes them close to being equal and reduces the formation of porosity and the growth of grains to give them more homogeneity.

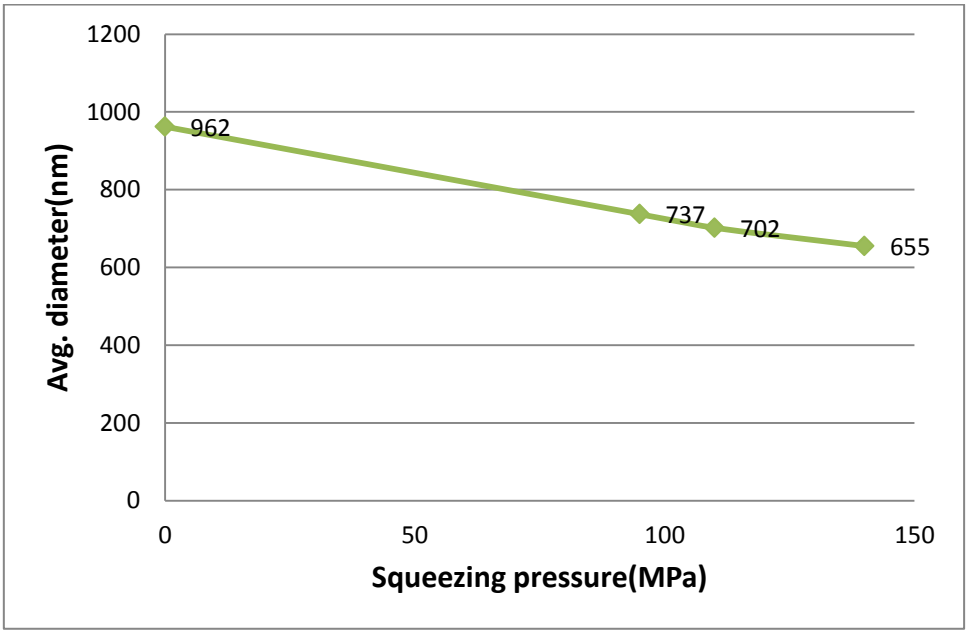

Figure (4.6)**:** The Rate of Decrease in Grain Size with Warm Squeezing

4.3.5 Density Measurement:

The density of the samples was measured prior to and after applying the squeezing process. The results are depicted in Fig. (4.7). The figure demonstrates an increase in density following the application of squeezing. Squeezing applied on the sample reduces the gaps (if any) between the grains, thus the density increases, and the increased density leads to the enhancement of the mechanical properties of the alloy. This rise in density can be attributed to plastic deformation and structural changes that occur when the material is subjected to squeezing. These

changes can cause particles within the material to rearrange or crystals to interlock, thereby influencing the atomic arrangement of the alloy and resulting in a density alteration. The standard value of the density is 2.81g/cm^3 [84], this confirms the positive effect of squeezing pressure.

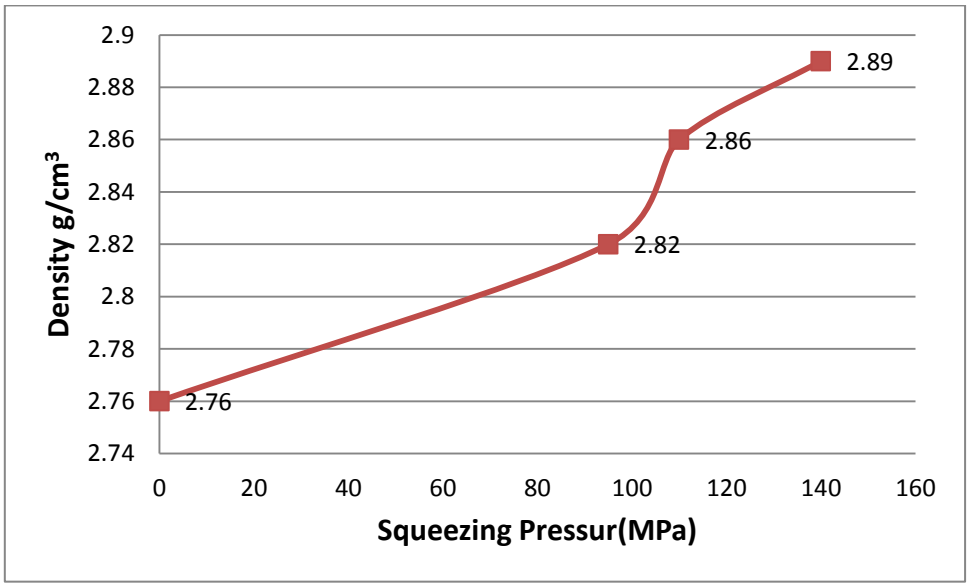

Figure (4.7)**:** The Effect of Warm Squeezing on the Density of the Alloy

4.3.6 Porosity Results:

Porosity test analysis is an important technique for characterizing the quality of alloys, as porosity can greatly affect the mechanical and physical properties of a material. The results in Figure.(4.8) show that the sample exposed to warm squeezing has lower porosity and higher density compared to the sample that was not subjected to warm squeezing. This process is used to modify the microstructure by causing plastic deformation and grain refinement, thus reducing the formation of porosity.

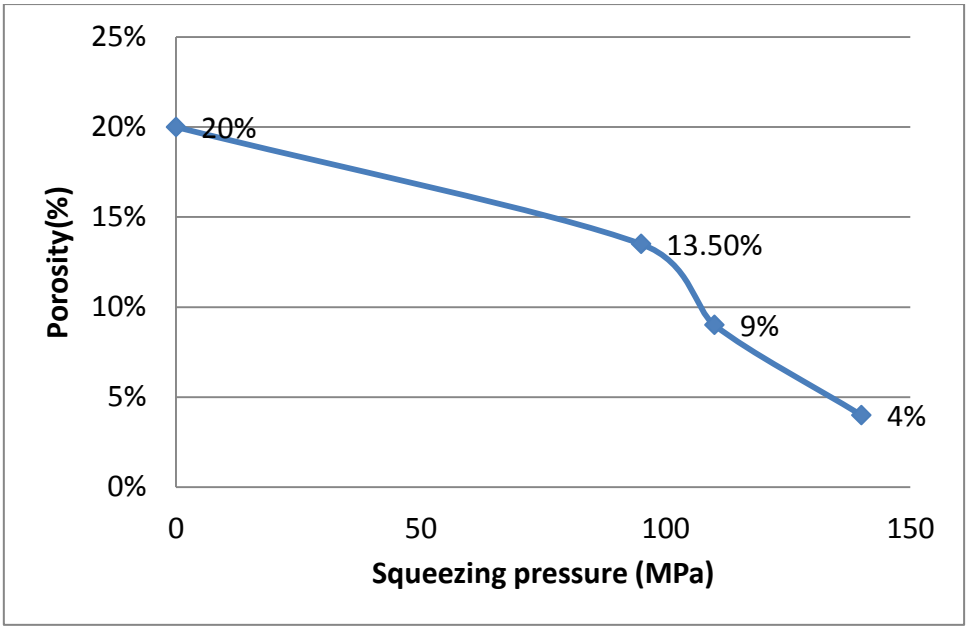

Figure (4.8)**:** The effect of Warm Squeezing on the Porosity

4.3.7 Hardness Results:

During warm squeezing, the material undergoes plastic deformation and structural changes. Such changes can lead to rearrangement of atoms and the formation of dislocations inside the crystal structure, and the temperature helps to facilitate the movement of atoms and dislocations, promote their rearrangement and create a more accurate and refined microstructure. This refined microstructure contributes to the enhancement of the hardness of the alloy.

The combination of plastic deformation, structural changes and improvement of the microstructure through warm squeezing allows 7075 aluminum alloy to achieve higher hardness levels than those usually obtained through other manufacturing processes. The standard values of the hardness of Vickers and Brinell are 175VH and150BH[37].

It should be noted that the specific parameters of the warm squeezing process, such as temperature, pressure and duration, must be carefully controlled and optimized to achieve the required hardness improvements while avoiding any possible adverse effects on the mechanical properties of the alloy.

The Brinell and Vickers hardness test was performed on five samples Fig.(4.9) shows the increase in the amount of hardness after each operation carried out on the sample.

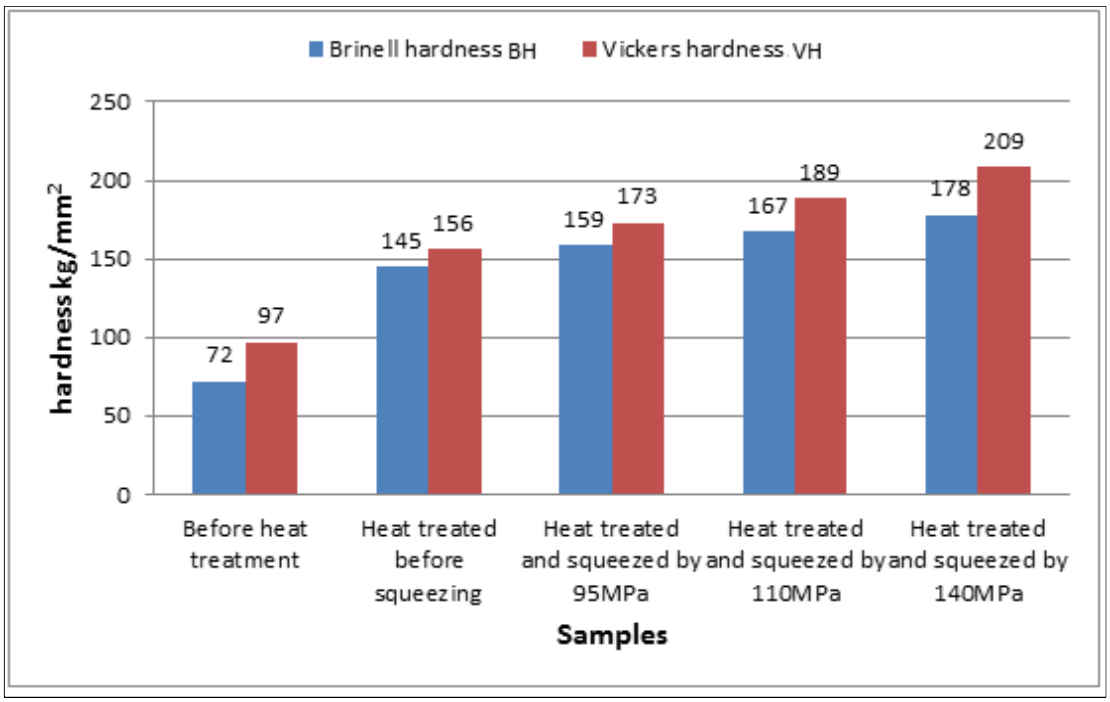

Figure (4.9)**:** Brinell and Vickers Hardness for all Samples

4.3.8 Tensile test Measurement:

Tensile testing of heat-treated and warm squeezed 7075Al alloy includes conducting a standard tensile test on the alloy, in addition to conducting a standard tensile test on the alloy with exposure to different thermal conditions for warm squeezed samples, the purpose of heat is to

change the mechanical properties and microstructure and evaluate its effect on the mechanical behavior of the alloy. data such as maximum tensile strength, yield strength and elongation shown are recorded in Table (4.3).

Table (4.3)**:** Results of the Tensile Tests

sample	**Temperature of the test °C**	**Ultimate Tensile Strength (MPa)**	**Elongation (%)**	**Yield Point (MPa)**
Heat treated	20	565	11.2	507
Heat treated and squeezed by 140**MPa**	20	674	40	583
Heat treated and squeezed by 140**MPa**	200	473	61.4	387
Heat treated and squeezed by 140**MPa**	250	390	93.7	300
Heat treated and squeezed by 140**MPa**	300	345	190.2	237
Heat treated	300	310	162.8	211

These values provide an insight into the mechanical behavior and strength of heat-treated and warm squeezed aluminum alloys, noting that the tensile strength of the standard alloy is 575MPa[37]. Figure (4.10) shows the samples before and after the test.

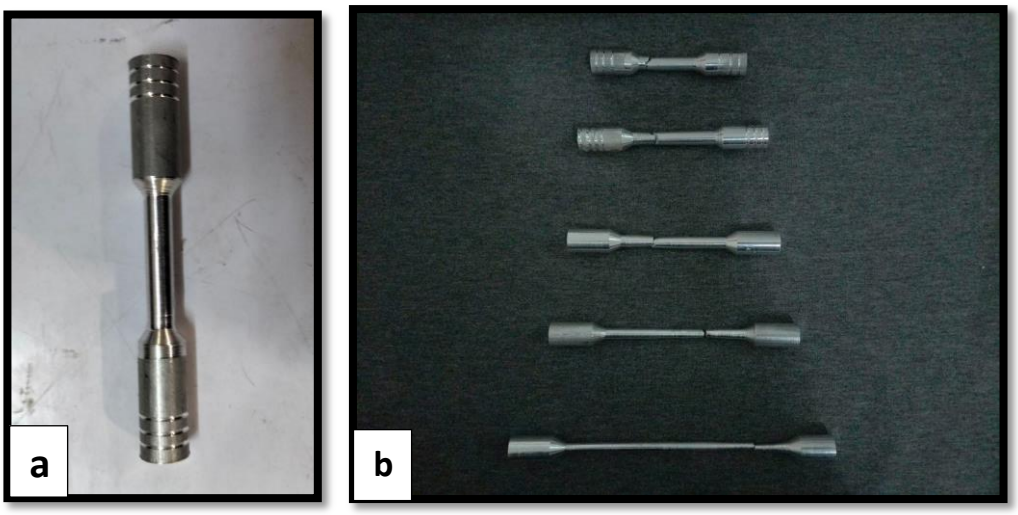

Figure (4.10): Tensile Specimen (a): Before Testing (b): After Testing

Through the test results, it is clear how the tensile strength increases and the elongation increases for the sample exposed to warm squeezing, while the elongation increases and the tensile strength decreases when the testing temperatures gradually increased, Figure (4.11) shows the stress-strain curve for laboratory samples.

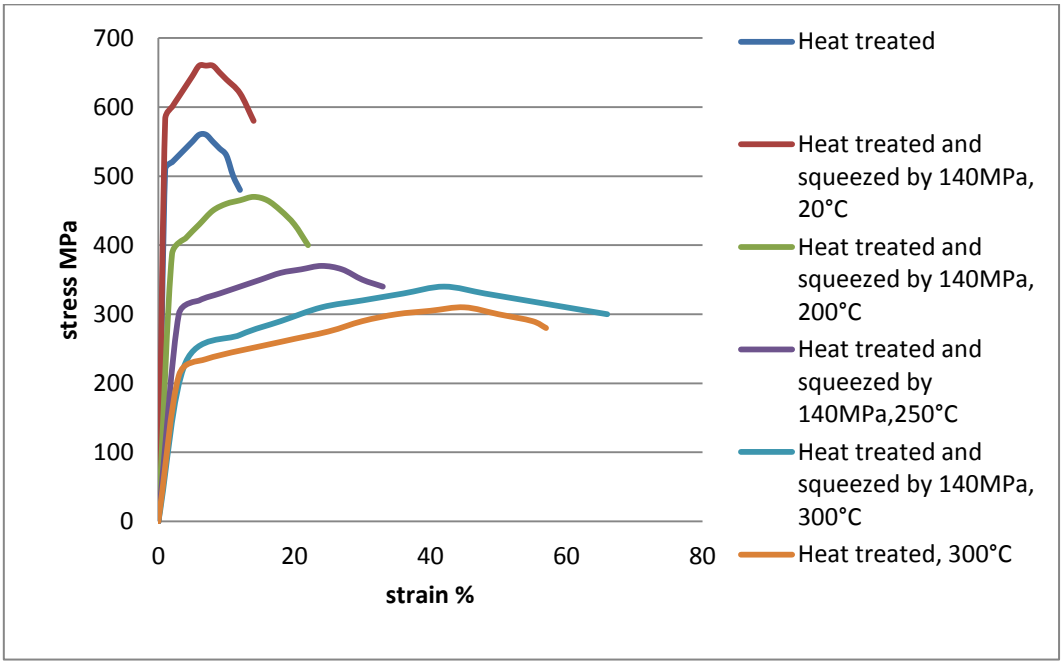

Figure (4.11): The Stress-strain Curve for Laboratory Samples

The elongation of the two samples, one of which underwent heat treatment and the other was subjected to warm squeezing, exhibits a notable disparity when tested at a temperature of 300 degrees. This discrepancy can be attributed to the squeezing process, which effectively reduces grain size, closes pores, and enhances the density of the alloy by eliminating voids and defects. Consequently, the susceptibility to crack initiation and propagation decreases, as warm squeezing promotes uniform deformation throughout the alloy. Additionally, it aids in redistributing strain and stress, minimizing the likelihood of localized deformation and improving the overall consistency of the deformable material.

4.3.9 Fracture Shape Analysis:

The examination of the fracture's form provides valuable insights into the material's properties such as tensile strength, elasticity, and energy absorption capacity prior to failure. By employing electron microscopy to scrutinize the fracture surface due to the tensile test, distinct features and indications can be identified, shedding light on the fracture type and material behavior. In the laboratory samples, visual evidence confirms the presence of granule displacement across the surface due to accumulated plastic deformations resulting from the applied tensile force, as illustrated in Figure (4.12).

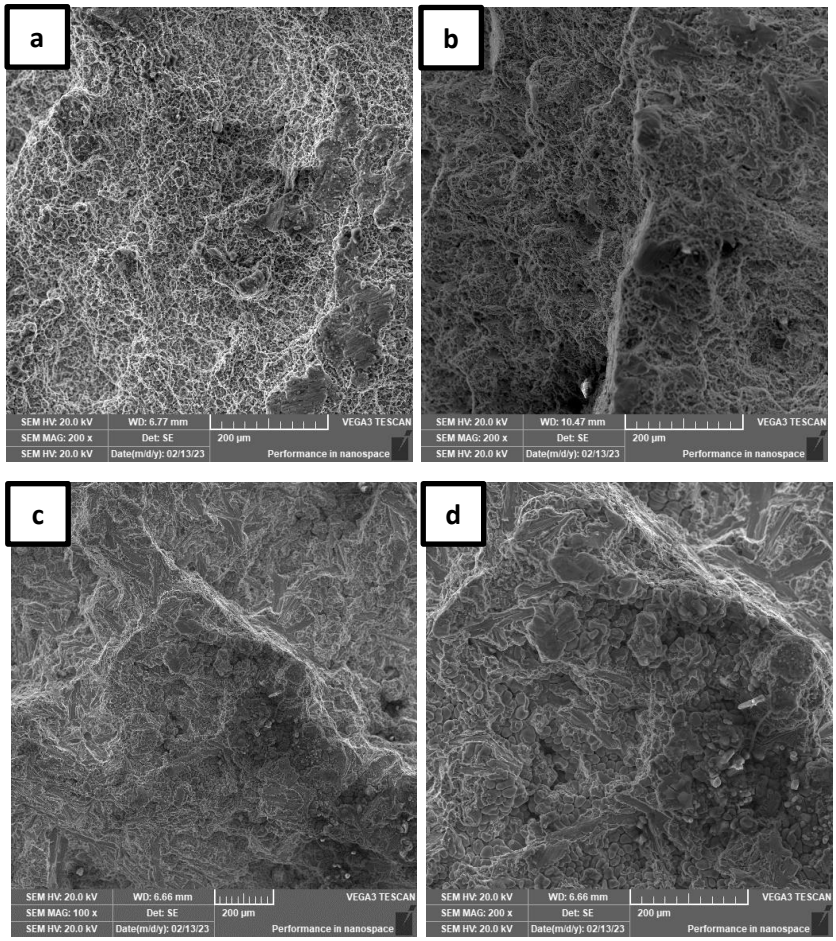

Figure (4.12)**:** Images of the Fracture Shape : (a) Heat Treated and Tested at 20°C; (b) Heat Treated, Squeezed by 140MPa and Tested at 20°C; (c) Heat Treated and Tested at 300°C; (d) Heat Treated, Squeezed by 140MPa and Tested at 300°C

The fracture takes the form of a tilted shear fracture at an angle, caused by extensive deformation. The angle of the fracture corresponds to the inclination of the fracture plane in relation to the plane perpendicular to the direction of tension. For the samples tested at the ambient and at the elevated temp., the angle is minimal for heat-treated and squeezed samples due to their strength and uniformity, while it is greater for heat-treated samples that have not undergone squeezing due to internal flaws.

4.3.10 Cutting Force Analysis:

Two models were taken for the analysis of cutting forces, the first is heat-treated only, the second is heat-treated and exposed to the warm squeezing with a pressure of (140 MPa) at (120°C). Through the results, the observed that the warm squeezing increased the cutting force due to the reduction of the internal defects and improvement of the crystal structure. Figures (4.13) and (4.14) show the change in cutting forces before and after the warm squeezing process.

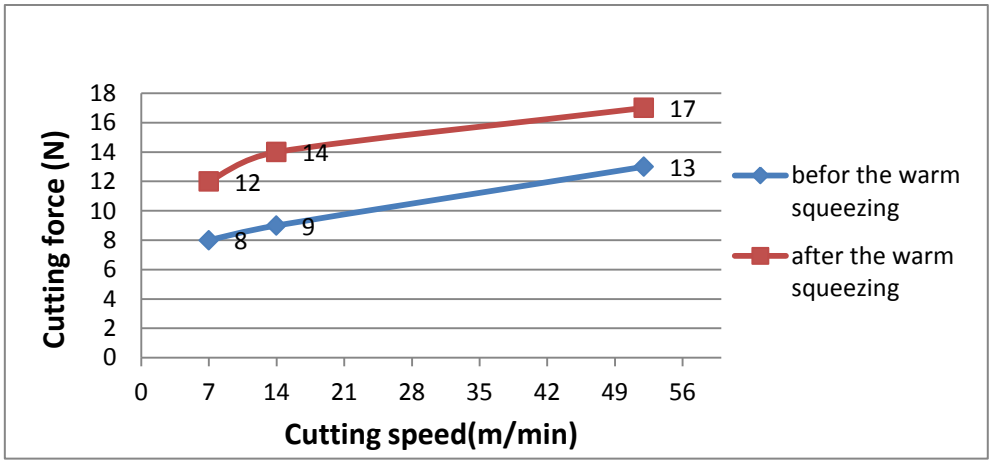

Figures (4.13)**:** Change of Cutting Force before and after Warm Squeezing at a Feed of 0.130 mm/rev

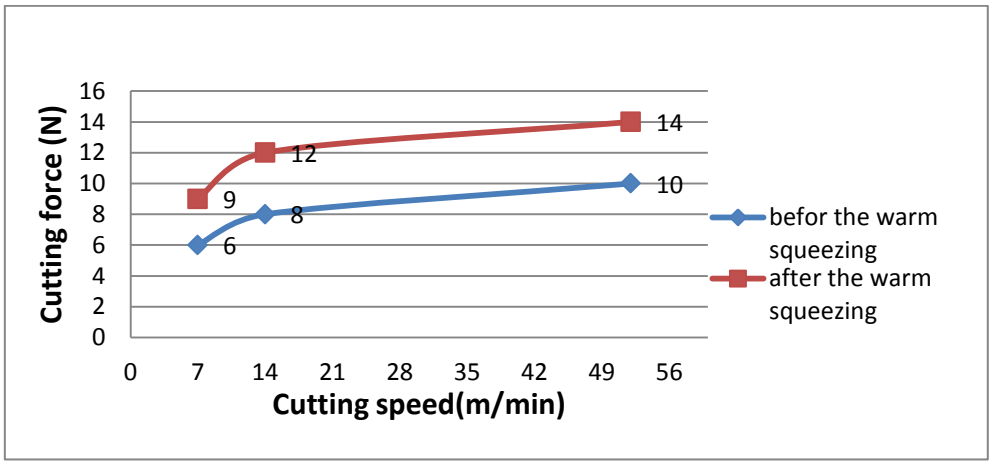

Figures (4.14)**:** Change of Cutting Force before and after Warm Squeezing at a Feed of 0.70 mm/rev

The reduction of internal defects, such as voids, inclusions, or impurities, is a significant benefit of warm squeezing. As the material is compressed, these defects tend to close or become more uniformly distributed, resulting in a more homogeneous material. This reduction in internal defects enhances the material's mechanical properties, including its strength, ductility, and toughness. Additionally, warm squeezing can lead to the refinement of the crystal structure. The high compressive forces applied during the process cause the material's grains to deform and rearrange. This results in a more refined grain structure, with smaller grain sizes and improved grain boundaries. A refined crystal structure improves the material's mechanical properties and provides better resistance to deformation, enhancing its overall strength.

In summary, warm squeezing can increase cutting force during machining due to the reduction of internal defects and the improvement of the crystal structure. These enhancements in material properties lead to improved strength and homogeneity, but they can also affect the machining process by requiring higher forces for material removal.

4.3.11 Results of Surface Roughness:

Raising the cutting speed can enhance surface quality and decrease the roughness of alloys. There are mechanisms that elucidate this phenomenon, as higher speed facilitates the more efficient removal of thin sections on the tool. Furthermore, an increase in cutting speed corresponds to a faster tool movement across the work surface, resulting in reduced friction and heat generation. Consequently, this decrease in friction and heat can mitigate combustion and heat-induced deformations that may negatively impact surface quality[85]. Figures (4.15) and (4.16)

show the difference in roughness and its contrast between the two samples tested before and after the warm squeezing. The sample subjected to the squeezing has improved surface roughness due to the reduction in porosity and gaps in the alloy, which led to a significant reduction in roughness.

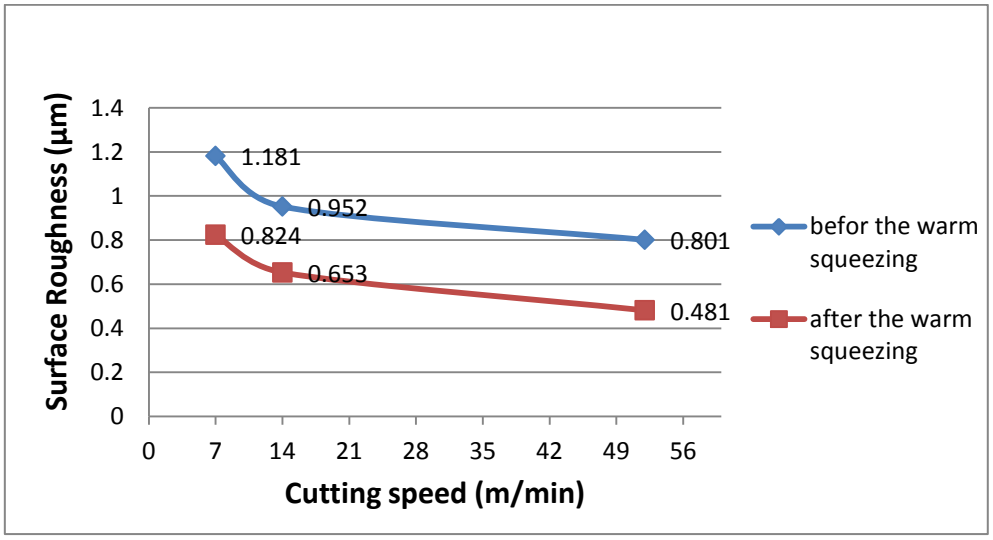

Figures (4.15)**:** Effect of Cutting Speed on Sample Surface Roughness before and after the Warm Squeezing Used at a Cutting Depth t= 0.2 mm and a Feed of (0.130 mm/rev)

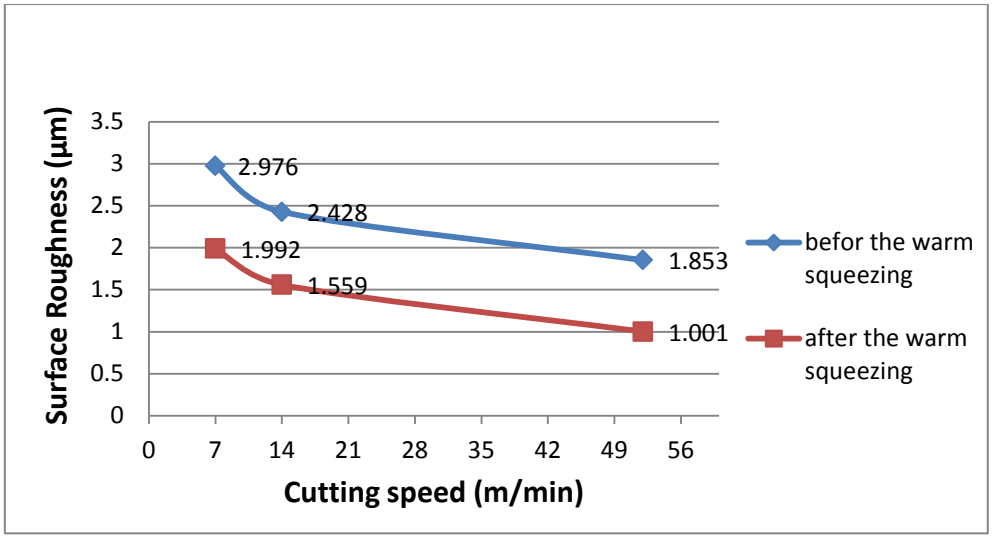

Figures (4.16)**:** Effect of Cutting Speed on Sample Surface Roughness before and after the Warm Squeezing Used at a Cutting Depth t = 0.2 mm and a Feed of (0.70 mm/rev)

It should be observed that when the feeding rate is raised, there is an associated rise in the rate of surface roughness. This can be attributed to various factors, including heightened cutting force exerted on the tool. Consequently, as the feeding rate increases, the roughness also increases. Moreover, an elevated feeding rate results in greater vibrations during operation. Additionally, an increase in the feeding rate may lead to increased pressure on the work piece and elevated temperature of the piece. These factors can contribute to the formation of metal films or alterations in the mechanical properties of the material, thereby leading to an escalation in surface roughness[86].

4.3.12 chip shape analysis:

The analysis of chip formation and its effect on the machinability of an alloy is crucial in understanding the machining process and choosing the cutting parameters for efficient and effective operations.

The morphology of the chips formed during machining provides valuable information about the machinability of the alloy. The chip shape, size, and color can indicate the nature of the cutting process and the interaction between the tool and the workpiece. Long, continuous chips generally indicate good machinability, while fragmented or discontinuous chips may suggest challenges in the machining process[87].

The presence of chip segmentation, where the chip breaks into separate segments during the machining process, can affect machinability. Segmented chips can cause issues such as poor surface finish, increased cutting forces, and reduced tool life. Proper chip control is essential for ensuring smooth and efficient machining operations. Uncontrolled chip formation can lead to problems like chip entanglement, chip recutting, and tool damage. The Table (4.4) indicates the test samples and the machining conditions followed.

Figure (4.17) shows the shapes of the chip formed for the two samples before and after warm squeezing when using three cutting speeds with two feed rates at a constant cutting depth.

Table(4.4)**:** Sample Type with Its Symbol, Cutting Speed and Feeding Used

Sample	Sample code	Vc(m/min)	Feed(mm/rev)
Before squeezing	S0	7	0.130
	S1	14	
	S2	52	
	S3	7	0.70
	S4	14	
	S5	52	
After squeezing by 140MPa at 120°C	S6	7	0.130
	S7	14	
	S8	52	
	S9	7	0.70
	S10	14	
	S11	52	

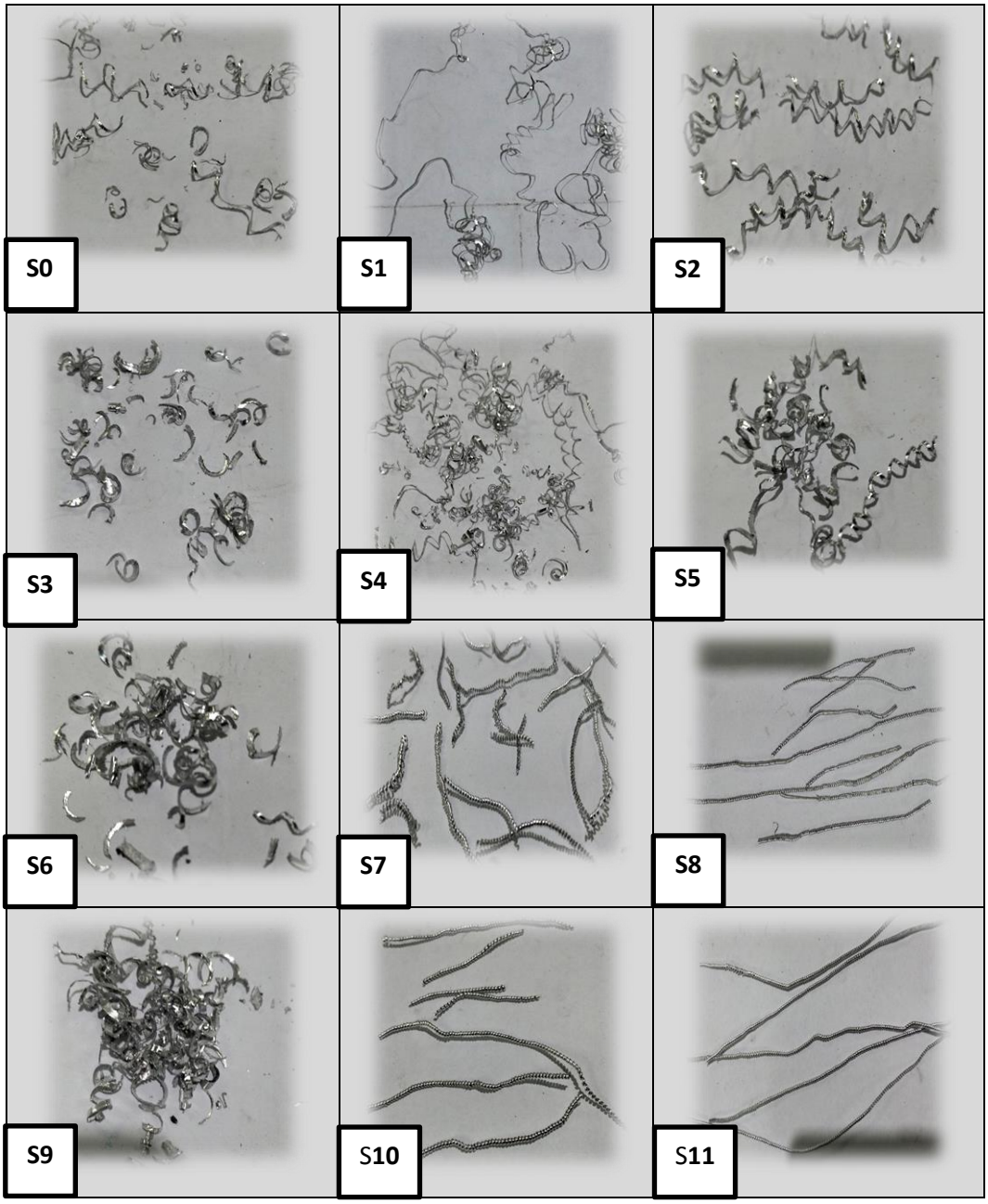

Figure (4.17)**:** Shows the Shapes of the Chip Formed

As the cutting velocity increases, the chips appearance changes, losing their fine quality and suggesting that higher cutting speeds produce thicker chips. When the feeding rate goes up, the chips can become distorted and discretions. Particularly, higher feed rates can result in chips getting tangled or cracked. Furthermore, applying warm squeezing

helps create a more continuous chips by reducing the grain size, and the porosity, which means increasing the toughness of the alloy sample[88].

Chapter Five

Chapter Five

Conclusions& Recommendations

5.1 Conclusions

The obtained data was used to analyze the findings, which are summarized as follows:

1-The warm squeezing process facilitates grain refinement in aluminium alloy 7075, leading to a finer grain structure

2-One of the main effects of warm squeezing on the superplasticity of aluminium 7075 is to improve the elongation percentage. Warm squeezing enhances deformation uniformity in the alloy and helps to redistribute stress and strain, reduce the possibility of local deformation and improve the overall consistency of the material's response to deformation. This is desirable for applications that require shaping or forming complex geometries.

3-The heat-treated alloy, when subjected to warm squeezing, demonstrated improved mechanical properties. This included a significant increase in both Brinell and Vickers hardness by 20% and 40% respectively. The density of the alloy also increased by 7%, while the porosity decreased by 80%. Additionally, the average diameter of the grains decreased by 32%.

4-The elongation percentage of the heat-treated sample increased by 40% with warm squeezing at 140 MPa. Furthermore, the elongation percentage increased during the tensile test at temperatures of 200, 250, and 300°C by 62%, 94%, and 191% respectively for the squeezed

sample. For the heat-treated sample alone, the elongation rate increased to 162% during the tensile test at a temperature of 300°C. This is attributed to the formation of a more uniform crystal structure, resulting in a higher density by eliminating porosity, voids, and other defects in the alloy. As a result, structural integrity is improved, reducing the susceptibility to crack initiation and propagation.

5-Due to the application of warm squeeze, the characteristics of the machining process were enhanced, resulting in a reduction of surface roughness by 67% and an increase in cutting force by 33%.

5.2 Recommendations

1-Conduct experimentation to determine the ideal temperature, pressure, and duration of warm squeezing that would yield the desired improvements in machining and mechanical properties of the 7075 aluminium alloy.

2- proper control of heat distribution during warm squeezing to avoid localized overheating or thermal gradients.

3-It is possible to study other mechanical qualities of 7075 aluminium alloy and improve them, such as fatigue resistance, where it's important to note that the specific improvement techniques and approaches may vary depending on the application, desired performance, and manufacturing constraints. Conducting further research, consulting with materials engineers, and performing testing and analysis can provide more detailed insights and recommendations for enhancing the fatigue resistance of 7075 aluminium alloy.

Reference

Reference.

[1] Adhikari, S., Tathavadkar, V., & Basu, B. (2022). Aluminium As a Structural Material. In Future Landscape of Structural Materials in India (pp. 25-43). Singapore: Springer Nature Singapore.

[2] B. Chatterjee and S. Bhowmik, "Evolution of material selection in commercial aviation industry—a review," Sustain. Eng. Prod. Manuf. Technol., pp. 199–219, Jan. 2019, doi: 10.1016/B978-0-12-816564-5.00009-8.

[3] R. Mohanraj, S. Elangovan, and S. Pratheesh Kumar, "Experimental investigations of warm incremental sheet forming process on magnesium AZ31 and aluminium 6061 alloy," Proc. Inst. Mech. Eng. Part L J. Mater. Des. Appl., vol. 237, no. 2, pp. 283–300, 2023.

[4] S. Salarieh, S. Nourouzi, and H. Jamshidi Aval, "An investigation on the microstructure and mechanical properties of Al-Zn-Mg-Cu/Ti composite produced by compocasting," Int. J. Met., vol. 16, no. 3, pp. 1397–1414, 2022.

[5] R. Ulewicz, K. Czerwińska, and A. Pacana, "A Rank Model of Casting Non-Conformity Detection Methods in the Context of Industry 4.0," Materials (Basel)., vol. 16, no. 2, p. 723, 2023.

[6] G. Wu, F. Chen, Z. Cui, and J. Zhang, "Manufacturing of fine-grained structures by multilevel kinking mechanism through a novel periodic undulating compression method: An example 7075 aluminum alloy," Int. J. Mach. Tools Manuf., vol. 182, p. 103953, 2022.

[7] E. Sáenz de Argandoña, L. Galdos, R. Ortubay, J. Mendiguren, and X. Agirretxe, "Room temperature forming of AA7075 aluminum alloys: W-temper process," in Key Engineering Materials, 2015, vol. 651, pp. 199–204.

[8] "Comparative Study to the Effect of Warm Forming and Mold vibration on the Microstructure of Al-Base Alloy," 2020.

[9] N. C. G. Silveira, M. L. F. Martins, A. Bezerra, and F. G. S. Araújo, “Red mud from the aluminium industry: production, characteristics, and alternative applications in construction materials—a review,” Sustainability, vol. 13, no. 22, p. 12741, 2021.

[10] K. Bulavskis, I. Adijāns, and L. Lazov, “Research of possibilities of laser polishing of the surface of aluminum,” in human. environment. technologies. Proceedings of the Students International Scientific and Practical Conference, 2021, no. 25, pp. 139–144.

[11] C. Shao, S. Zhao, X. Wang, Y. Zhu, Z. Zhang, and R. O. Ritchie, “Architecture of high-strength aluminum–matrix composites processed by a novel microcasting technique,” NPG Asia Mater., vol. 11, no. 1, p. 69, 2019.

[12] L. Wang et al., “Plasma electrolytic oxidation coatings on additively manufactured aluminum–silicon alloys with superior tribological performance,” Surf. Coatings Technol., vol. 435, p. 128246, 2022.

[13] L. W. Zahner, Aluminum Surfaces: A Guide to Alloys, Finishes, Fabrication and Maintenance in Architecture and Art. John Wiley & Sons, 2019.

[14] M. Ozesmi, T. E. Patiroglu, G. Hillerdal, and C. Ozesmi, “Peritoneal mesothelioma and malignant lymphoma in mice caused by fibrous zeolite,” Br. J. Ind. Med., vol. 42, no. 11, pp. 746–749, 1985, doi: 10.1136/oem.42.11.746.

[15] H. R. Kotadia, G. Gibbons, A. Das, and P. D. Howes, “A review of Laser Powder Bed Fusion Additive Manufacturing of aluminium alloys: Microstructure and properties,” Addit. Manuf., vol. 46, p. 102155, 2021.

[16] P. Rambabu, N. Eswara Prasad, V. V Kutumbarao, and R. J. H.

Wanhill, “Aluminium alloys for aerospace applications,” Aerosp. Mater. Mater. Technol. Vol. 1 Aerosp. Mater., pp. 29–52, 2017.

[17] N. B. S. MONOGRAPH, “Stress Corrosion Cracking Control Measures”.

[18] B. Chakravarthi, “Buckling and mold analysis of connection rod with different materials using ansys.” Andhra university, 2022.

[19] Y. Li et al., “Al alloys and casting processes for induction motor applications in battery-powered electric vehicles: A review,” Metals (Basel)., vol. 12, no. 2, p. 216, 2022.

[20] Z. Wang et al., “Selective laser melting of aluminum and its alloys,” Materials (Basel)., vol. 13, no. 20, p. 4564, 2020.

[21] M. Nicolas, “Precipitation evolution in an Al-Zn-Mg alloy during non-isothermal heat treatments and in the heat-affected zone of welded joints.” Institut National Polytechnique de Grenoble-INPG, 2002.

[22] D. Godard, “Influences de la précipitation sur le comportement thermomécanique lors de la trempe d’un alliage Al-Zn-Mg-Cu.” Institut National Polytechnique de Lorraine, 1999.

[23] M. Hansen, K. Anderko, and H. W. Salzberg, “Constitution of binary alloys,” J. Electrochem. Soc., vol. 105, no. 12, p. 260C, 1958.

[24] H. Y. Hunsicker and H. C. Stumpf, “History of Precipitation Hardening, Sorby Centennial Symposium on the History of Metallurgy,” New York Gordon Breach Sci. Publ., vol. 8, p. 234, 1965.

[25] G. E. Totten and D. S. MacKenzie, Handbook of aluminum: vol. 1: physical metallurgy and processes, vol. 1. CRC press, 2003.

[26] S. Gadea and M. Protopopescu, “Non-ferrous alloys.” Technical Edit., Bucharest, 1965.

[27] J. L. Murray,(1980), “Bulletin of Alloy Phase Diagrams “ National Bureau of Standards Vol. 4 No. 1 19

[28] I. J. Polmear, “The ageing characteristics of ternary aluminium-zinc-magnesium alloys,” J. Inst. Met., vol. 86, 1957.

[29] H. A. Youssef, H. A. El-Hofy, and M. H. Ahmed, Manufacturing technology: materials, processes, and equipment. Crc Press, 2011.

[30] M. Nicolas, “Precipitation evolution in an Al-Zn-Mg alloy during non-isothermal heat treatments and in the heat-affected zone of welded joints.” Institut National Polytechnique de Grenoble-INPG, 2002

[31] P. K. Mandal, “Heat treatment and friction stir processing effects on mechanical properties and microstructural evolution of sc inoculated Al-Zn-Mg alloys,” Mater. Sci. Met. Eng, vol. 4, pp. 16–28, 2017.

[32]Aaronson, H. I., Enomoto, M., & Lee, J. K. (2016). Mechanisms of diffusional phase transformations in metals and alloys. CRC Press.

[33] H. Y. Hunsicker and H. C. Stumpf, “History of Precipitation Hardening, Sorby Centennial Symposium on the History of Metallurgy,” New York Gordon Breach Sci. Publ., vol. 8, p. 234, 1965.

[34] Fultz, B. (2020). Phase transitions in materials. Cambridge University Press.

[35] Kermanidis, A. T. (2020). Aircraft aluminum alloys: applications and future trends. Revolutionizing Aircraft Materials and Processes, 21-55.

[36]Leenaers, A. (2014). Surface-engineered low-enriched Uranium-Molybdenum fuel for research reactors. University of Ghent-SCK• CEN.

[37] G. E. Totten and D. S. MacKenzie, Handbook of aluminum: vol. 1: physical metallurgy and processes, vol. 1. CRC press, 2003.

[38] G. Giuliano, Superplastic forming of advanced metallic materials: methods and applications. Elsevier, 2011.

[39] W. A. Backofen, “Superplasticity in an Al-Zn alloy,” Trans. Asm, vol. 57, pp. 980–990, 1964.
[40] H. A. Youssef, H. A. El-Hofy, and M. H. Ahmed, Manufacturing technology: materials, processes, and equipment. Crc Press, 2011.
[41] G. E. Dieter, “Mechanical Metallurgy McGraw Hill Book Company,” New York, 1961.
[42] O. D. Sherby and J. Wadsworth, “Superplasticity—Recent advances and future directions,” Prog. Mater. Sci., vol. 33, no. 3, pp. 169–221, 1989.
[43] T. G. Nieh, L. M. Hsiung, J. Wadsworth, and R. Kaibyshev, “High strain rate superplasticity in a continuously recrystallized Al–6% Mg–0.3% Sc alloy,” Acta Mater., vol. 46, no. 8, pp. 2789–2800, 1998.
[44] K. V. Rajulapati, “Synthesis and mechanical properties of two phase nanostructured Al based composites,” 2007.
[45] C. Geng, H. Zhang, X. Li, and H. Geng, “Elevated temperature tensile behaviour of 5183 aluminium alloy made by electrospark deposition additive manufacturing,” Mater. Sci. Eng. A, vol. 868, p. 144746, 2023.
[46] R. B. Figueiredo and T. G. Langdon, “Deformation mechanisms in ultrafine-grained metals with an emphasis on the Hall–Petch relationship and strain rate sensitivity,” J. Mater. Res. Technol., vol. 14, pp. 137–159, 2021.
[47] Y. Li, S. Hu, E. Barker, N. Overman, S. Whalen, and S. Mathaudhu, “Effect of grain structure and strain rate on dynamic recrystallization and deformation behavior: A phase field-crystal plasticity model,” Comput. Mater. Sci., vol. 180, p. 109707, 2020.
[48] P. Trusov, N. Kondratev, and A. Podsedertsev, “Grain Structure

Rearrangement by Means the Advanced Statistical Model Modified for Describing Dynamic Recrystallization," Metals (Basel)., vol. 13, no. 1, p. 113, 2023.

[49] R. J. Immanuel, S. K. Panigrahi, and J. C. Malas, "Materials development for sustainable manufacturing," in Sustainable Manufacturing Processes, Elsevier, 2023, pp. 155–194.

[50] P. B. Prangnell and C. P. Heason, "Grain structure formation during friction stir welding observed by the 'stop action technique,'" Acta Mater., vol. 53, no. 11, pp. 3179–3192, 2005.

[51] O. Gutfleisch, "Controlling the properties of high energy density permanent magnetic materials by different processing routes," J. Phys. D. Appl. Phys., vol. 33, no. 17, p. R157, 2000.

[52] A. Bachmaier and R. Pippan, "High-pressure torsion deformation induced phase transformations and formations: new material combinations and advanced properties," Mater. Trans., vol. 60, no. 7, pp. 1256–1269, 2019.

[53] Q. Tan et al., "Demonstrating the roles of solute and nucleant in grain refinement of additively manufactured aluminium alloys," Addit. Manuf., vol. 49, p. 102516, 2022.

[54] V. Satheeshkumar, R. G. Narayanan, and J. S. Gunasekera, "Sustainable manufacturing: material forming and joining," in Sustainable Manufacturing Processes, Elsevier, 2023, pp. 53–112.

[55] K. Edalati et al., "Nanomaterials by severe plastic deformation: review of historical developments and recent advances," Mater. Res. Lett., vol. 10, no. 4, pp. 163–256, 2022.

[56] R. Z. Valiev, B. Straumal, and T. G. Langdon, “Using severe plastic deformation to produce nanostructured materials with superior properties,” Annu. Rev. Mater. Res., vol. 52, pp. 357–382, 2022.

[57] M. Kawasaki and T. G. Langdon, “The development of internal cavitation in a superplastic zinc–aluminum alloy processed by ECAP,” J. Mater. Sci., vol. 43, pp. 7360–7365, 2008.

[58] Kasaeian-Naeini, M., Sedighi, M., & Hashemi, R. (2022). Severe plastic deformation (SPD) of biodegradable magnesium alloys and composites: A review of developments and prospects. Journal of Magnesium and Alloys, 10(4), 938-955.

[59] S. Mohd Yusuf, S. Cutler, and N. Gao, “The impact of metal additive manufacturing on the aerospace industry,” Metals (Basel)., vol. 9, no. 12, p. 1286, 2019.

[60] W. König and D. Erinski, “Machining and machinability of aluminium cast alloys,” CIRP Ann., vol. 32, no. 2, pp. 535–540, 1983.

[61] M. M. Tash, F. H. Samuel, and S. Alkahtani, “Machinability of Heat-Treated 356 and 319 Aluminum Alloys: Methodology for Data Processing and Calculation of Drilling Force and Moment,” in Advanced Materials Research, 2012, vol. 396, pp. 1008–1022.

[62] P. Roy, S. K. Sarangi, A. Ghosh, and A. K. Chattopadhyay, “Machinability study of pure aluminium and Al–12% Si alloys against uncoated and coated carbide inserts,” Int. J. Refract. Met. Hard Mater., vol. 27, no. 3, pp. 535–544, 2009.

[63] H. Demir and S. Gündüz, “The effects of aging on machinability of 6061 aluminium alloy,” Mater. Des., vol. 30, no. 5, pp. 1480–1483, 2009.

[64] V. Songmene, R. Khettabi, I. Zaghbani, J. Kouam, and A. Djebara,

“Machining and machinability of aluminum alloys,” Alum. Alloy. Theory Appl, vol. 377, p. 400, 2011.

[65] G. Campatelli and A. Scippa, “Prediction of milling cutting force coefficients for Aluminum 6082-T4,” Procedia Cirp, vol. 1, pp. 563–568, 2012.

[66] X. Zhang, H. Mu, X. Huang, Z. Fu, D. Zhu, and H. Ding, “Cryogenic milling of aluminium-lithium alloys: thermo-mechanical modelling towards fine-tuning of part surface residual stress,” Procedia Cirp, vol. 31, pp. 160–165, 2015.

[67] N. Fang and Q. Wu, “The effects of chamfered and honed tool edge geometry in machining of three aluminum alloys,” Int. J. Mach. Tools Manuf., vol. 45, no. 10, pp. 1178–1187, 2005.

[68] P. Zhang, Z. Liu, J. Liu, J. Yu, Q. Mai, and X. Yue, “Effect of aging plus cryogenic treatment on the machinability of 7075 aluminum alloy,” Vacuum, vol. 208, p. 111692, 2023.

[69] Q. Tan et al., “A novel strategy to additively manufacture 7075 aluminium alloy with selective laser melting,” Mater. Sci. Eng. A, vol. 821, p. 141638, 2021.

[70] S. R. Zaidi, M. Khan, S. H. I. Jaffery, and S. Warsi, “Effect of Machining Parameters on Surface Roughness During Milling Operation,” Adv. Manuf. Technol, vol. 15, pp. 175–180, 2021.

[71] Kannan, C., & Ramanujam, R. (2017). Comparative study on the mechanical and microstructural characterisation of AA 7075 nano and hybrid nanocomposites produced by stir and squeeze casting. Journal of advanced research, 8(4), 309-319.

[72] Agarwal, P., Kishore, A., Kumar, V., Soni, S. K., & Thomas, B. (2019). Fabrication and machinability analysis of squeeze cast Al 7075/h-BN/graphene hybrid nanocomposite. Engineering Research Express, 1(1), 015004

[73] Al-Ethari, H., Radhi, N. S., & Hamzah, S. A. (2020). Influence of Mechanical and Thermo Mechanical Treatment on Micro Structure and Hardness of Al-Zn-Mg Alloy. Test engineering & management, 0193-4120 Page No. 11133 - 11141

[74] Österreicher, J. A., Tunes, M. A., Grabner, F., Arnoldt, A., Kremmer, T., Pogatscher, S., & Schlögl, C. M. (2020). Warm-forming of pre-aged Al-Zn-Mg-Cu alloy sheet. Materials & Design, 193, 108837.

[75] Hua, L., Hu, X., & Han, X. (2020). Microstructure evolution of annealed 7075 aluminum alloy and its influence on room-temperature plasticity. Materials & Design, 196, 109192.

[76] Soni, S. K., & Thomas, B. (2020). Microstructure, mechanical properties and machinability studies of Al7075/SiC/h-BN hybrid nanocomposite fabricated via ultrasonic-assisted squeeze casting. FME Transactions, 48(3), 532-542.

[77] Rajesh, S., Kumar, R. S., Madhankumar, S., Sheshan, M., Vignesh, M., & Kumar, R. S. (2021). Study of the mechanical properties of Al7075 alloy, silicon carbide and fly ash composites manufactured by stir casting technique. Materials Today: Proceedings, 45, 6438-6443.

[78] Wang, K., Hu, S., Wang, T., Xie, W., Guo, T., Li, F., & Luo, R. (2022). Microstructural Evolution and Mechanical Properties of 7075 Aluminium Alloy during Semi-Solid Compression Deformation. Crystals, 12(8), 1119.

[79] Parakh, A., Lee, A. C., Chariton, S., Wang, M. M., Kiani, M. T., Prakapenka, V. B., & Gu, X. W. (2022). High pressure induced precipitation in Al7075 alloy. arXiv preprint arXiv:2202.01203.

[80] N. Verma and S. C. Vettivel, “Characterization and experimental analysis of boron carbide and rice husk ash reinforced AA7075 aluminium alloy hybrid composite,” J. Alloys Compd., vol. 741, pp. 981–998, 2018.

[81] ASTM Committee. (2013). Standard test methods for density and specific gravity (relative density) of plastics by displacement: ASTM D792—2013.

[82] S. Invernizzi, F. Montagnoli, and A. Carpinteri, “Experimental evidence of specimen-size effects on EN-AW6082 aluminum alloy in VHCF regime,” Appl. Sci., vol. 11, no. 9, p. 4272, 2021.

[83] Georgantzia, E., Gkantou, M., & Kamaris, G. S. (2021). Aluminium alloys as structural material: A review of research. Engineering Structures, 227, 111372.

[84] Ren, Y., Liu, H., Zhao, L., Cui, X., Shen, Y., Wang, J., & Xiong, T. (2021). Study of microstructural and mechanical anisotropy of 7075 Al deposits fabricated by cold spray additive manufacturing. Materials & Design, 212, 110271.

[85] Soren, T. R., Kumar, R., Panigrahi, I., Sahoo, A. K., Panda, A., & Das, R. K. (2019). Machinability behavior of aluminium alloys: A brief study. Materials Today: Proceedings, 18, 5069-5075.

[86] Liao, Z., la Monaca, A., Murray, J., Speidel, A., Ushmaev, D., Clare, A., ... & M'Saoubi, R. (2021). Surface integrity in metal machining-Part I: Fundamentals of surface characteristics and formation mechanisms. International Journal of Machine Tools and Manufacture, 162, 103687.

[87] Rahman, M. A., Bhuiyan, M. S., Sharma, S., Kamal, M. S., Imtiaz, M. M., Alfaify, A., ... & Mia, M. (2021). Influence of feed rate response (FRR) on chip formation in micro and macro machining of al alloy. Metals, 11(1), 159.

[88] Sabbar, H. M., Leman, Z., Shamsudin, S. B., Tahir, S. M., Aiza Jaafar, C. N., Hanim, M. A. A., ... & Al-Alimi, S. (2021). AA7075-ZrO2 nanocomposites produced by the consecutive solid-state process: A review of characterisation and potential applications. Metals, 11(5), 805.

Appendix

X-ray Diffraction (XRD):

Name and formula

Reference code:	00-015-0228
Compound name:	Aluminum Magnesium Zinc
Empirical formula:	$AlMg_2Zn$
Chemical formula:	$AlMg_2Zn$

Crystallographic parameters

Crystal system:	Unknown
RIR:	-

Subfiles and Quality

Subfiles:	Alloy, metal or intermetalic Inorganic
Quality:	Doubtful (O)

Comments

Creation Date:	01/01/1970
Modification Date:	01/01/1970
Chemical analysis (wt.%):	Zn 40, Mg 40, Al 20
Reason O Quality Was Assigned:	O was assigned because unindexed
Additional Diffraction Lines:	Plus 15 additional reflections to 1.092.

References

Primary reference: Clark., *Trans. Am. Soc. Met.*, **53**, 295, (1961)

Peak list

No.	h	k	l	d [A]	2Theta[deg]	I [%]
1				9.03000	9.787	10.0
2				7.76000	11.394	4.0
3				7.38000	11.983	16.0
4				5.20000	17.038	10.0
5				4.92000	18.015	4.0
6				4.62000	19.196	4.0
7				4.48000	19.801	4.0
8				4.31000	20.591	12.0
9				4.23000	20.985	6.0
10				4.08000	21.765	8.0
11				3.97000	22.376	4.0
12				3.83000	23.205	16.0
13				3.56000	24.993	6.0
14				3.20000	27.858	4.0
15				3.08000	28.967	4.0
16				2.99000	29.858	4.0
17				2.81000	31.820	2.0
18				2.69000	33.280	2.0
19				2.65000	33.797	2.0
20				2.58000	34.743	10.0
21				2.49000	36.041	40.0
22				2.44000	36.806	100.0
23				2.42000	37.121	60.0
24				2.36000	38.101	20.0
25				2.31000	38.958	18.0
26				2.22000	40.606	14.0
27				2.21000	40.798	20.0
28				2.19000	41.187	16.0
29				2.13000	42.402	25.0
30				2.10500	42.931	16.0
31				2.06000	43.917	16.0
32				2.04600	44.233	14.0
33				2.00000	45.306	6.0
34				1.98000	45.790	6.0
35				1.95000	46.535	8.0
36				1.85000	49.212	4.0
37				1.79700	50.765	1.0
38				1.78700	51.069	1.0
39				1.73000	52.880	1.0

Stick Pattern

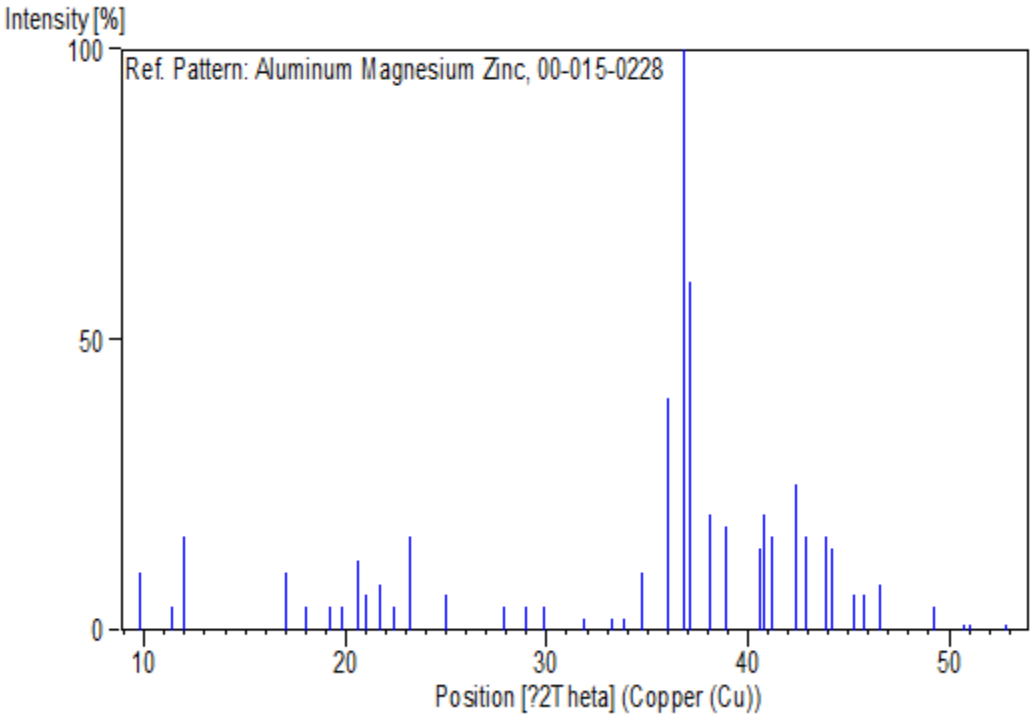

Name and formula

Reference code:	00-039-0951
Compound name:	Aluminum Magnesium Zinc
Empirical formula:	$Al_{49}Mg_{32}$
Chemical formula:	Mg_{32} (Al, Zn)$_{49}$

Crystallographic parameters

Crystal system:	Unknown
RIR:	-

Subfiles and Quality

Subfiles:	Alloy, metal or intermetalic Inorganic
Quality:	Doubtful (O)

Comments

Creation Date:	01/01/1970
Modification Date:	01/01/1970
Icosahedral point group symmetry. Reason O Quality Was Assigned:	O was assigned because unindexed
Sample Preparation:	Produced by rapid quenching.

References

Primary reference: Rajasekharan, T., Akhtar, D., Gopalan, R., Muraleedharan, K., *Nature (London)*, **322**, 528, (1986)

Peak list

No.	h	k	l	d [A]	2Theta[deg]	I [%]
1				4.23000	20.985	5.0
2				3.74000	23.772	4.0
3				2.42300	37.073	51.0
4				2.29200	39.277	100.0
5				2.12900	42.423	6.0
6				2.03200	44.554	23.0
7				1.77800	51.347	1.0
8				1.42800	65.289	19.0
9				1.35100	69.524	2.0
10				1.22400	78.001	4.0
11				1.21700	78.536	1.0

Stick Pattern

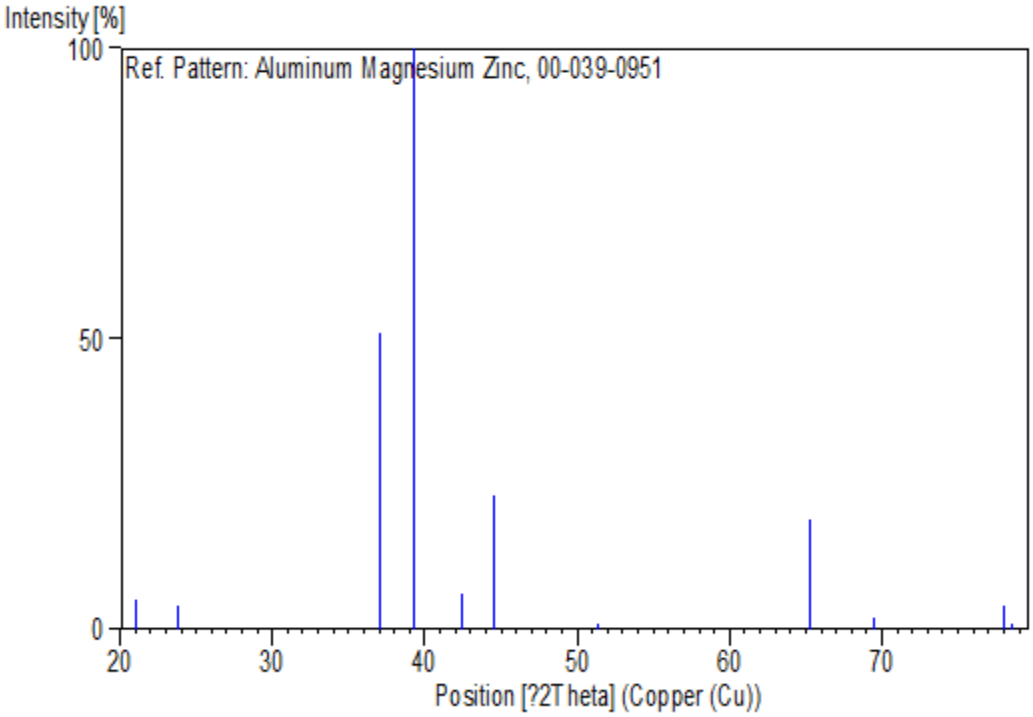
Intensity [%]
100
50
0
Ref. Pattern: Aluminum Magnesium Zinc, 00-039-0951
20
30
40
50
60
70
Position [?2Theta] (Copper (Cu))

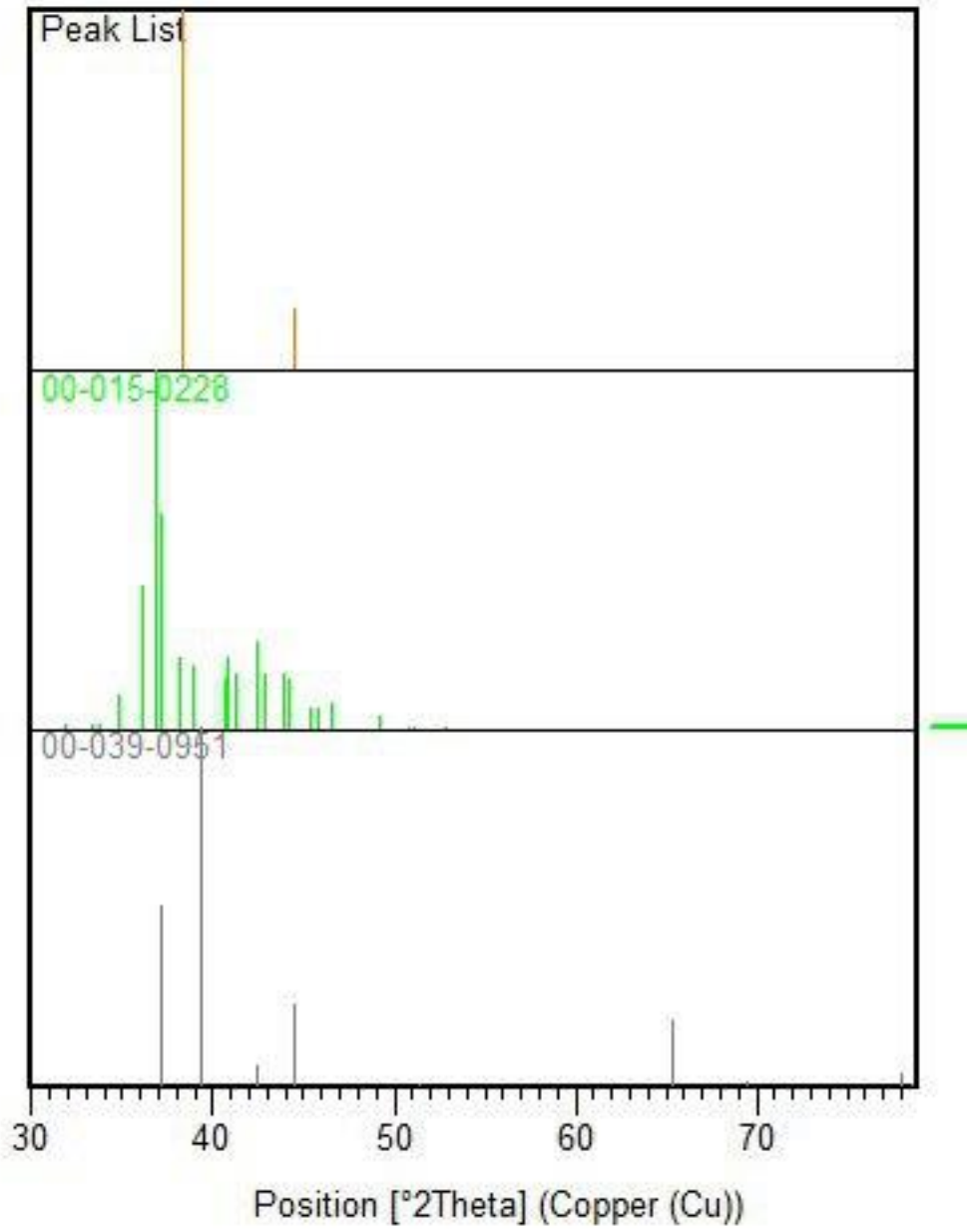
Peak List
00-015-0228
00-039-0951
30
40
50
60
70
Position [°2Theta] (Copper (Cu))